15 Anomalous Earthquake Ruptures at Shallow Depths on Subduction Zone Megathrusts

Thorne Lay and Susan Bilek

Abstract

Interplate thrust faults in subduction zones host the largest earthquakes and majority of seismic energy release on Earth. The seismically coupled portion of these megathrusts typically extends 100 ± 50 km across the depth range from 5–10 to 25–55 km, with convergent motions between underthrusting and overriding plates being accommodated by a mixture of earthquake slip, postseismic deformation, and interseismic creep. There are varying proportions of seismic and aseismic slip distributed with depth and varying seismic coupling coefficients in different subduction zones. Rupture of the shallow portion of megathrusts is the focus of this review; both large and small thrust earthquakes in the upper 10 km of the seismogenic zone sometimes display unusual seismic energy release attributes, with low rupture velocity and/or low stress drop. The largest of these events can be exceptionally tsunamigenic, with seismic slip extending updip of the apparent seismic front defined by smaller events. The transition from aseismic stable sliding on the shallow megathrust contact with any sedimentary wedge to the unstable slip regime of the seismically coupled zone at greater depth is variable from region to region and may involve zones of conditional stability that display bimodal deformation behavior as strain rates fluctuate. Systematic variations of rupture process with depth across the upper 10 km of the seismogenic regime have been observed, suggesting depth dependence of mechanical properties of the megathrust that may provide key information about sediment induration, hydrothermal processes, and frictional behavior of the megathrust. The acute seismic faulting heterogeneity observed in the shallow megathrust complicates generalization about the environment based on isolated spatial sampling of its properties, but there is great need for in situ ground truth determinations of structures and properties in the shallow megathrust.

Introduction

Subduction of oceanic lithosphere occurs along massive interplate thrust faults that are the contact surfaces between overriding and underthrusting plates in convergent margins. These megathrusts accommodate the convergent motions by varying portions of seismic and aseismic slip, with significant variations in geometry and maximum earthquake size from region to region [e.g., *Kanamori*, 1977; *Uyeda and Kanamori*, 1979; *Ruff and Kanamori*, 1980; *Pacheco et al*., 1993; *Scholz and Campos*, 1995]. About 90% of the seismic moment released by global earthquakes occurs near subduction zones, with most events involving slip on megathrusts, including the largest recorded events, the 1960 Chile and 1964 Alaska earthquakes [e.g., *Pacheco and Sykes*, 1992]. The important tectonic role played by megathrusts has prompted many efforts to characterize their seismic and aseismic properties, including the depth extent of interplate faulting, variations in maximum earthquake size, and the underlying causes of faulting complexity observed for individual ruptures.

The updip and downdip bounds on interplate seismic slip (fig. 15.1) are generally located near depths of ~5–10 and 25–55 km below the seafloor, respectively [e.g., *Byrne et al.,* 1988; *Hyndman et al*., 1995, 1997; *Oleskevich et al*., 1999; *Tichelaar and Ruff*, 1991, 1993; *Zhang and Schwartz*, 1992; *Pacheco et al*., 1993; *Suárez and Sánchez*, 1996; *Deshon et al*., 2003]. The updip limit usually involves a transition from stable-sliding to unstable stick-slip behavior [e.g., *Marone and Saffer*, this volume], commonly below a shallow tapering sedimentary wedge, at a lateral distance of 20–100+ km from the trench called the "seismic front" [e.g., *Yoshii*, 1979; *Marone and Scholz*, 1988; *Pacheco et al*., 1993], although earthquake ruptures may extend right to the trench when little sediment is present [e.g., *Polet and Kanamori*, 2000]. Temperatures at the updip limit are estimated as around 100°–150°C [e.g., *Hyndman et al*., 1997]. A variety of mechanisms likely control the downdip edge of the seismically coupled zone, which is typically at temperatures from ~350°–450°C. Thermal control on the frictional mechanism at the downdip edge in the case of subduction of relatively young oceanic crust, or transition in the fore-arc mantle to weak, serpentinized wedge material for island arcs and for subduction of older oceanic crust, has been proposed by *Tichelaar and Ruff* [1993], *Hyndman and Wang* [1993], *Hyndman et al*. [1997], and *Peacock and Hyndman* [1999]. The overall seismogenic depth extent and dip angle define the maximum width available for the largest earthquake ruptures that can occur in each subduction zone, with widths ranging from 50 to 150 km [*Pacheco et al*., 1993]. A few regions with flattened megathrusts tend to have broader fault widths and larger megathrust earthquakes [e.g., *Gutscher and Peacock*, 2003].

Studies of the largest earthquakes along megathrusts in different subduction zones have suggested some correlations with convergence rate, lithospheric age, sediment supply, bathymetric features, and back-arc spreading [e.g., *Ruff and Kanamori*, 1980, 1983b; *Peterson and Seno*, 1984; *Jarrard*, 1986; *Ruff*,

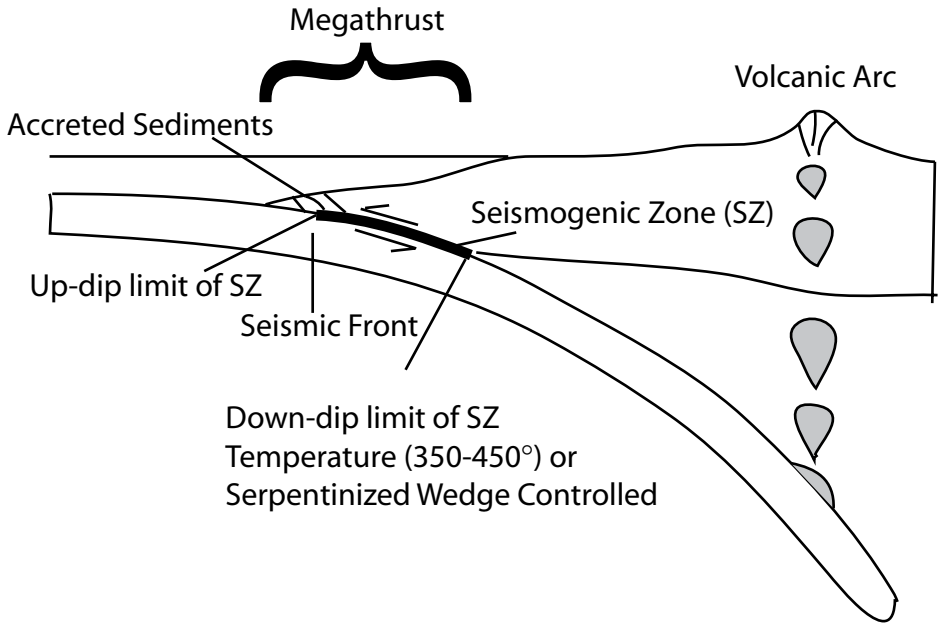

Figure 15.1 Schematic diagram illustrating the megathrust fault in subduction zones at approximately correct scale. The thick black line highlights the seismogenic range of the megathrust on which large thrust earthquakes occur. This has an updip limit and a downdip limit controlled by a variety of processes. Below the downdip limit earthquakes occur only within the subducting slab as intraplate faulting. The nature of the upper plate, the amount of accreted sediments, and the geometry of the megathrust vary from region to region as described in the text. The shallow portion of the seismically coupled megathrust is the focus of this review.

1989; *van der Hilst and Seno*, 1993; *Pacheco et al*., 1993; *Scholz and Campos*, 1995]. While gross physical attributes of subduction zone environments may affect the width of the seismogenic interface and maximum earthquake size, the statistics are not particularly compelling with regard to any overall model [e.g., *Pacheco et al*., 1993]. One of the more prominent trends is that when back-arc spreading is pronounced, the largest megathrust events tend to be smaller [e.g., *Kanamori*, 1977; *Uyeda and Kanamori*, 1979; *Scholz and Campos*, 1995].

The substantial variations between earthquake ruptures within an individual subduction zone and from event to event for repeated failures of a given region of a megathrust have prompted numerous studies. Notions of variable fault zone failure strength, and resultant seismic slip heterogeneity, such as the asperity model [e.g., *Lay and Kanamori*, 1981; *Lay et al*., 1982; *Ruff and Kanamori*, 1983b; *Kanamori*, 1986; *Schwartz and Ruff*, 1987; *Ruff*, 1992; *Ruff and Miller*, 1994], emerged from studies of subevents of large ruptures. *Scholz* [1990, 1998] discusses frictional perspectives of such rupture heterogeneity, arguing that it is

more useful to invoke notions of stable and unstable sliding, with observed rupture complexity arising from variations in state variables such as effective normal stress, temperature from frictional heating, and material properties such as rock and sediment composition, permeability, and roughness.

It is generally recognized that significant interplate slip must occur aseismically, even within the seismogenic depth range, to account for total plate convergence in most subduction zones [e.g., *Ruff and Kanamori*, 1983a; *Peterson and Seno*, 1984; *Pacheco et al*., 1993; *Scholz and Campos*, 1995]. Precise determination of seismic coupling is statistically difficult given the short historic record available [*McCaffrey*, 1997], but the current evidence favors a full range of seismic coupling values from 0 (purely aseismic subduction) to 1 (purely seismic subduction). Regions such as Kamchatka, Alaska, South Chile, East Aleutians, West Aleutians, and Nankai have high seismic coupling coefficients, while the Marianas, Kermadec, South Tonga, Izu Bonin, Java, North Peru, Vanuatu, and Central America have low seismic coupling [e.g., *Scholz and Campos*, 1995].

The depth distribution of interplate thrusting along the megathrust has been explored in an effort to understand this seismic coupling variability [e.g., *Zhang and Schwartz*, 1992; *Pacheco et al*., 1993]. Most subduction zones exhibit peaked distributions of earthquake numbers and moment release as functions of depth, tapering toward both updip and downdip limits of the seismogenic zone. The data suggest that a relatively narrow portion of the seismogenic zone tends to have the highest proportion of seismic coupling, and even this may be laterally "patchy" [e.g., *Pacheco et al*., 1993]. Localized asperity regions may undergo purely seismic slip, corresponding to total seismic coupling, thereby controlling overall failure process of the megathrust [e.g., *Lay et al*., 1982; *Thatcher*, 1989]. Seamounts, horst and graben structures, and other bathymetric features on the underthrusting plate may account for locally enhanced frictional contacts [e.g., *Kelleher and McCann*, 1976; *Cloos*, 1992; *Pacheco et al*., 1993; *Cloos and Shreve*, 1996; *Scholtz and Small*, 1997; *Tanioka et al*., 1997; *von Huene et al*., 1999; *Abercrombie et al*., 2001; *Husen et al*., 2002; *Bilek*, this volume], or these features may provide barriers that delimit rupture [e.g., *Kodaira et al*., 2000; *Hirata et al*., 2003], but as yet there is not a good understanding of the nature of the localized high-slip regions for interplate events or of the persistence of such features over time [e.g., *Scholz*, 1990; *Thatcher*, 1990].

The apparent complexity of sliding properties of the megathrust is even more pronounced in the shallowest region, <15 km below the ocean bottom. This region generally has a higher ratio of aseismic to seismic slip than the deeper interface and is likely to have acute variations in physical properties due to the presence of indurating sediments, expelled fluids, rough bathymetric structure on the subducting plate, complex structure of the overriding wedge, and vulnerability to transient high strain rates upon failure of the deeper interface. This review will focus on the seismological observations of earthquakes at shallow depths on the megathrust, considering first large, then smaller events, to assess possible constraints on this complex environment.

Large Earthquakes on the Shallow Megathrust

Systematic investigations of the rupture processes of interplate thrust events have identified high-slip regions within the rupture zones for most of the very large events that have occurred during the past 50 years or so [e.g., *Schwartz and Ruff*, 1987; *Kikuchi and Fukao*, 1987; *Beck and Ruff*, 1989; *Ruff and Miller*, 1994]. In almost all cases the primary slip occurs in the depth range 15–40 km, with relatively few documented instances of large slip extending to shallower depths, even after allowing for substantial uncertainties in subevent locations. Studies of the depth distribution of underthrusting events larger than magnitude 5 or so during the past 25 years show that relatively few events tend to occur in the shallowest part of the seismogenic zone [e.g., *Zhang and Schwartz*, 1992; *Pacheco et al*., 1993]. These observations are generally attributed to the shallow portion of the megathrust undergoing a transition from stable sliding to unstable friction as depth increases, possibly with an intervening zone of conditional stability [*Scholz*, 1998]. Subduction of low permeability, water-saturated clays could increase fluid pressures in the shallow fault zone, lowering the effective normal stress and allowing stable sliding to depths of 5–10 km. Anelastic deformation of weak, unconsolidated fore-arc sediments in contact with the megathrust at very shallow depth could also play a role [e.g., *McCaffrey*, 1993]. Given ongoing motion of the underthrusting plate due to combined forces from slab-pull and ridge-push, large, elastic shear strains would not be expected to accumulate along the shallow megathrust as its frictional properties accommodate the deformation by stable sliding. High strain-rate loading caused by sudden failure of the deeper unstable sliding regime would not always induce large slip in any conditionally stable region at shallow depth and the shallowest region of any velocity-strengthening material would quickly terminate any slip event. These general considerations are at odds with the observation that in some locations the shallow portion of the megathrust actually has failed in large earthquakes, with very large slip, both with and without failure of the deeper portion of the rupture zone. When this occurs, resulting displacements of the seafloor are large, generating strong tsunamis, in a special class of earthquakes called tsunami earthquakes.

The 1896 and 1946 Tsunami Earthquakes

Tsunami earthquakes were identified by *Kanamori* [1972] as a distinct class of seismic events for which the tsunami excitation was larger than expected given the measured seismic magnitude (usually, the 20-s surface wave magnitude M_s). He considered two underthrusting events notable for their great tsunamis: The 1896 Sanriku (M_s 7.2) and 1946 Aleutian (M_s 7.4) events (fig. 15.2). The global tsunami magnitudes M_t estimated for these events by *Abe* [1979] are 8.6 and 9.3, respectively, so there are huge differences between M_s and M_t,

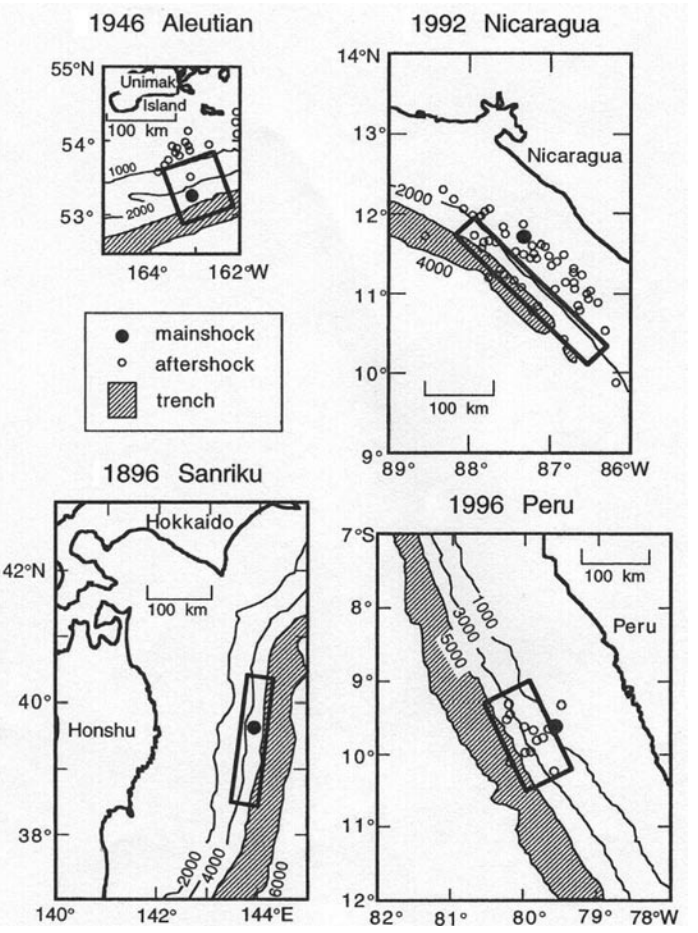

Figure 15.2 Fault models for four tsunami earthquakes: the 1946 Aleutian [*Johnson and Satake*, 1997], 1896 Sanriku [*Tanioka and Satake*, 1996a], 1992 Nicaragua [*Satake*, 1994] and 1996 Peru [*Satake and Tanioka*, 1999] events. Bathymetry is shown with contour lines. Boxes outline fault models used by the various authors. [From *Satake and Tanioka*, 1999].

distinguishing these from typical events. The limited seismic data available for these events yield effective seismic moment determinations that increase greatly with increasing period, indicative of source process time constants of ~100 s [*Kanamori*, 1972]. At long periods the discrepancy between seismic source strength and tsunami magnitude is thus greatly reduced, suggesting that faulting displacements may be able to account for the strong tsunami excitation without need for additional effects such as submarine slumping. Both events have locations relatively close to their respective trenches. *Kanamori* [1972] suggested that the long rupture durations of these events are related to

weakness in the source zones, possibly associated with reduction of strength in the thrust zone due to nearby normal faulting in the oceanic plate.

Subsequent investigations of the tsunami data for the 1896 event confirm that the source area is very close to the trench, 210 km long, and ~50 km in width (fig. 15.2) [*Tanioka and Satake*, 1996a]. Slip of 5.7 m (for a dip angle of 20°) near the trench was estimated, a surprisingly large amount of slip to occur at very shallow depth along the Honshu coast. Rupture in low-rigidity sediments was suggested as a mechanism to give low rupture velocity (which can account for the long source process time) and resultant weak excitation of 20-s surface waves. Using a relatively low rigidity of 20 GPa based on observations of sediments being subducted (at greater depth around the plate interface it is common to assume a "hard rock" rigidity of 50 GPa), *Tanioka and Satake* [1996a] estimated a moment magnitude, M_w, of 8.0; still lower than the global tsunami magnitude of 8.6 or even the local tsunami magnitude of 8.2 [*Abe*, 1981]. Using a more realistic dip angle of ~10° requires a slip of 10.4 m, increasing the estimated M_w to 8.2 [*Tanioka and Seno*, 2001], and reducing, but not eliminating, the $M_w - M_t$ discrepancy without violating any seismic constraints. Even lower dip angles can be reconciled with regional microearthquakes [*Umino et al*., 1995], so some of the difference between seismic and tsunami magnitudes can be accounted for. Very shallow dip angles for thrust faults lead to poor excitation of long-period seismic waves, but tsunami excitation is not as dependent on source depth or dip angle [*Ward*, 1982], so reducing dip of the shallow megathrust goes in the right direction to account for the relative tsunami excitation. *Tanioka and Seno* [2001] sought to further reconcile the seismic and tsunami strength estimates by accounting for possible lateral plowing and uplift of the very small sedimentary wedge seaward of the slip zone [e.g., *Seno*, 2000], an effect that can enhance tsunami excitation by ~50% because of broadened ocean bottom uplift that results. This reduces the slip needed at depth for a 10° dipping fault, lowering the M_w back to 8.0–8.1, but predicting some of the contrast to M_t.

The 1946 event produced a truly remarkable tsunami, which caused a 30-m local run-up on Unimak Island and 16-m run-up in Hawaii. The tide gauge recordings for this event were studied in detail by *Johnson and Satake* [1997]. Using a 100-km-long rupture based on the aftershock distribution [*Sykes*, 1971], an estimate of 9.6–9.8 m of slip was obtained to match the tsunami records, with strong slip extending up to the trench, seaward of the aftershock zone (fig. 15.2). A limited set of body waves analyzed by *Pelayo* [1990] yielded a 90-s duration source time function, suggesting a very slow rupture velocity of <1 km/s. For an assumed rigidity of 20 GPa, an M_w of 8.2–8.3 was estimated, still well below the M_t of 9.3, but *Johnson and Satake* [1997] argue that the latter value may be biased upward by harbor resonances. *Pelayo* [1990] estimated a very large seismic moment from surface wave spectra that gives an $M_w = 8.6$. This predicts a 27-m slip using a standard rigidity, but such a large slip overpredicts the early (pre-Harbor resonance) tsunami amplitudes. *Kanamori*

[1985] suggested that the focal mechanism for long period signals of the 1946 event may be best represented by a single force, implying that a landslide contributed to the tsunami excitation, as is preferred for the 1929 Grand Banks event [*Hasegawa and Kanamori*, 1987]; however, the model of *Johnson and Satake* [1997] indicates that the pre-Harbor resonance tsunami observations can be well explained by a megathrust faulting source with slow slip and rupture extending to the trench.

Tsunami Earthquakes Between 1960 and 1992

Following the initial study of the 1896 and 1946 tsunami earthquakes by *Kanamori* [1972], several smaller events with anomalous tsunami excitation were identified in the shallow megathrusts along the Kurile Islands and Peru. In particular, the 20 October 1963 (M_s 6.9) and 10 June 1975 (M_s 7.0) events in the Kurile subduction zone were classified as tsunami earthquakes [e.g., *Fukao*, 1979; *Ward*, 1982; *Pelayo and Wiens*, 1992], and the 20 November 1960 (M_s 6.75) tsunami event occurred along the Peru margin [*Pelayo and Wiens*, 1990]. The two events in the Kuriles locate seaward (updip) of large slip regions in the rupture zones of larger interplate thrusts along the megathrust [*Schwartz and Ruff*, 1987]. The aftershock zones overlap those of earlier great thrusts at depth but extend all the way to the trench. *Fukao* [1979] suggested that the Kurile events are very shallow, and their source process times are <100 s (unusually long, but insufficient to account for the discrepancy between M_s and tsunami strength). On the basis of some indications of change in focal mechanisms during rupture, he proposed that relatively steeply dipping splay faulting into the sedimentary wedge might account for strong ocean-bottom deformation needed to explain the tsunamis. Low rigidity μ of the sediments (13 GPa) was assumed, requiring ~ 4 times more slip at the source to give the same seismic moment, M_o. The seafloor deformation scales as $M_o/\mu = Ad$, where A is the fault area and d is the average displacement, thus large displacement and shallow depth would combine to give strong tsunami excitation [see *Okal*, 1988]. Splay fault branching into the accretionary wedge has also been suggested to occur along the Nankai subduction zone [*Cummins and Kaneda*, 2000; *Park et al*., 2002].

Pelayo and Wiens [1992] modeled P and SH waveforms for the Kurile events, favoring source depths <10 km with a smooth, broad, 90-s source function for the 20 October 1963 event and a 60-s duration pulse for the 10 June 1975 event, with both events having weak slip in the first 20 s or so. Shallow dips of 7°–8°, with no change in mechanism, were found. The 20 November 1960 Peru event was modeled as a shallow (5–25 km) thrust event with very shallow dip angle (6°) and a rupture duration of 110 s [*Pelayo and Wiens*, 1990]. For these three events the long source durations and moderate aftershock zone dimensions suggest low rupture velocities, but this was not directly determined because point-source models were used. *Pelayo and Wiens* [1992] conclude that all three events involve slow rupture along the basal décollement of the accretionary

prism, with low rigidity around the shallow megathrust being responsible for the low rupture velocities. The long source process time reduces M_s relative to M_o, leading to discrepancy between the tsunami size and M_s, as in the model of *Kanamori* [1972]. The very shallow source depths and shallow dip angles further reduce the seismic wave excitation relative to the tsunami excitation.

Tsunami Earthquakes of the Broadband Seismology Era

Several tsunami earthquakes have occurred subsequent to deployment of global networks of broadband seismic equipment; this has provided the opportunity for improved seismological characterization of their rupture processes. By far the most important of these events was the 1992 Nicaragua earthquake, which struck on 2 September in a seismic gap that had been identified by *Harlow et al*. [1981]. This event has an M_t = 7.9–8.0, and caused a 10-m tsunami run-up at the coastal village of El Transito and 2–6 m run-up along the entire Nicaraguan coast [*Satake et al*., 1993; *Ide et al*., 1993; *Imamura et al*., 1993], despite weak ground shaking (≤ Modified Mercalli III). The aftershock zone is 200 km long and ~100 km wide, an unusually large size for an M_s 7.2 event. A modest number of aftershocks locate close to the trench. *Ihmlé* [1994] relocated the aftershocks, finding that most events concentrate in a 40-km-wide zone ~250 km long, with an updip region ~50 km wide being almost devoid of aftershocks (fig. 15.2). The aftershock distribution has the appearance of a conventional seismic front, but as discussed below, it appears that the primary mainshock slip was updip of this region. *Ide et al*. [1993] and *Kanamori and Kikuchi* [1993] found that the surface wave radiation patterns for the Nicaragua event are consistent with a shallow underthrusting event rather than with a single force, so a landslide source is not favored. *Kanamori and Kikuchi* [1993] note that there is no sedimentary wedge off of Nicaragua, and they suggest that rupture propagated all the way to the trench with the megathrust frictional properties being affected by the subducted sediments.

The 256-s period surface wave moment magnitude for the Nicaragua event is M_w = 7.6 [*Ide et al*., 1993; *Kanamori and Kikuchi*, 1993], substantially larger than the M_s; this partly closes the gap with M_t. The rupture centroid time shift is ~50 s, suggesting a source duration of ~100 s [*Ide et al*., 1993; *Kanamori and Kikuchi*, 1993; *Velasco et al*., 1994]. The source process time estimated using a procedure similar to that which *Kanamori* [1972] applied to the 1896 and 1946 tsunami events, is 40% as long as for those earlier tsunami events [*Ide et al*., 1993]. *Kanamori and Kikuchi* [1993] find that the Nicaragua event did not have an increase in apparent seismic moment for periods longer than 200 s, which is also consistent with a shorter source process time than for the 1896 and 1946 events. This event thus appears to be similar to the 1960 Peru, 1963 Kurile Island, and 1975 Kurile Island events, but it generated far superior seismic data because of the increased bandwidth of global seismic recording stations.

Several investigations of the source time function for the 1992 Nicaragua event were undertaken using the broadband digital seismic data, including body and surface wave analyses [e.g., *Ide et al*., 1993; *Kanamori and Kikuchi*, 1993; *Satake et al*., 1993; *Velasco et al*., 1994; *Kikuchi and Kanamori*, 1995; *Ihmlé* 1996a, 1996b]. The data are abundant enough and have sufficient bandwidth to directly determine some aspects of the source rupture finiteness from directivity effects in the seismic waves, the first time this was possible for a tsunami earthquake. This is important, given that the aftershocks may not illuminate the updip region of the rupture zone if it has unusual frictional properties. The Nicaragua event commenced with a 10-s interval of low energy release, then ruptured updip and asymmetric bilaterally, with a rupture velocity of ~1.0–2.2 km/s [e.g., *Ide et al*., 1993; *Velasco et al*., 1994; *Kikuchi and Kanamori*, 1995; *Ihmlé*, 1996b], with slip distributed along a 160–200 km long fault length. The low-frequency centroid locations estimated for the overall energy release [*Dziewonski et al*., 1993; *Velasco et al*., 1994; *Ihmlé*, 1996b] are updip of the relocated aftershocks, suggesting that significant slip occurred in a region with no aftershocks [*Ihmlé*, 1996b]. The published slip models differ in slip distribution over the fault, apparently due to the smooth nature of the source time functions and intrinsic trade-offs between changes in rupture area expansion rate and slip. The early stage of slow energy release during the rupture complicates location of the regions of strong slip. The model parameterization (such as use of constant or variable rupture velocity) also has strong effects on the inferred slip distribution. There are also problems in recovering the body wave ground motion baselines associated with near-field terms visible in the unusually smooth teleseismic records [e.g., *Kanamori*, 1993; *Kikuchi and Kanamori*, 1995]. The slip models are consistent in having strong slip just northwest of the epicenter that dominates the early portion of the radiation, with slow southeastward expansion of the slip dominating the latter portion of the radiation. The seismic waveform data provide little direct constraint on the actual width of the rupture zone, but shallow centroid depths of 10 km or less are favored by *Dziewonski et al*. [1993] and *Velasco et al*. [1994].

Ide et al. [1993] estimated the static stress drop as 0.26 MPa for a rupture zone width of 100 km, a rigidity of 30 GPa, and average dislocation of 0.5 m. *Kikuchi and Kanamori* [1995] assumed a 50-km-wide rupture zone and obtained a static stress drop of 1.1 MPa with an average dislocation of 1.4 m for the same rigidity, along with estimating the average rise time of the dislocation to be ~10 s. The average dislocation velocity is thus estimated to be 0.14 m/s, significantly slower than for other subduction zone events. The seismic wave energy E_s to moment, M_o ratio was estimated as $E_s / M_o = 6.2 \times 10^{-7}$, about an order of magnitude lower than typical for earthquakes [e.g., *Choy and Boatwright*, 1995; *Ruff*, 1999]. The apparent stress, defined by $\sigma_a = 2\mu E_s / M_o = 0.037$ MPa, is much lower than the static stress drop. Using source time functions inferred from surface waves and the centroid-moment tensor moment of *Dziewonski et al*. [1993], *Velasco et al*. [1994] estimated the apparent stress as 0.03 MPa, so this result

is fairly stable for relatively uniform slip models. *Ihmlé* [1996b] found a more heterogeneous slip model, with two patches having average slips of 3.5–4.5 m (for assumed rigidity of 22 GPa). This gives higher localized static stress drop values of 3.0–7.0 MPa. Rise times of 10–18 s were preferred in the models of *Ihmlé* [1996b], so dislocation velocities of 0.2–0.7 m/s are estimated.

The tsunami observations for the Nicaragua event have been modeled by *Imamura et al*. [1993], *Titov and Synolakis* [1993], *Satake* [1994, 1995], *Piatanesi et al*. [1996], and *Geist and Bilek* [2001]. *Imamura et al*. [1993] used linear long-wave theory to study the tsunami propagation, with an assumed run-up ratio of 2. They found a uniform 3.75-m slip for assumed 200×100 km^2 fault area and rigidity of 30 GPa, giving a seismic moment one order of magnitude greater than observed. A similar result was found by *Titov and Synolakis* [1993], who included a one-dimensional nonlinear run up computation. The discrepancy with the seismic model was reduced to a factor of 5.6 by *Imamura et al*. [1993] by taking a smaller fault area of 150×75 km^2, although the larger fault area was slightly preferred by the authors. *Satake* [1994, 1995] modeled tide-gauge waveforms and run-up observations using linear shallow water equations and nonlinear equations including bottom friction and showed that the required fault width is actually only 40 km, much narrower than the aftershock area and extending only as deep as 10 km. Uniform slip over a 250-km-long fault was preferred, although a 200-km fault with larger slip at the southeastern end of the fault can match the data well (fig. 15.2). The slip needed for this model is 3 m, which can be reconciled with the seismic moment by using a rigidity of 10 GPa. *Piatanesi et al*. [1996] modeled the tsunami run-up data with a variable slip model, using a nonlinear shallow-water theory. A slip function intermediate between a uniform slip model and the variable slip model of *Ihmlé* [1996b] was preferred, with two predominant slip patches having slip of 3.5–4.5 m near the epicenter and at the southeastern end of the rupture zone, and slip elsewhere along the fault being 1–2 m. A rigidity of 10 GPa was assumed, with a 50×250 km long fault. *Geist and Bilek* [2001] further reconciled the seismic and tsunami models by using the slip model of *Ihmlé* [1996b] with a depth-dependent shear modulus [*Bilek and Lay*, 1998, 1999b] increasing from 3.6 to 30 GPa across the rupture plane, finding good agreement with the tide-gauge waveform at Corinto.

These studies, by far the most comprehensive for any tsunami earthquake, demonstrate that the best overall model for the 1992 Nicaraguan event involves shallow thrusting on a 40–50 km wide fault extending from the trench down to depths of no more than 10 km or so (fig. 15.2). Few aftershocks fall within the area of large slip (~3 m). There is no accretionary prism in the trench; thus it is assumed that sediments have been subducted. The overall rupture took ~110 s, commencing with 10 s of weak slip and then bilateral expansion over the fault zone at low slip velocities. The average source volume rigidity is ~10 GPa.

There has been one additional recent tsunami earthquake of note; the 21 February 1996 Peruvian earthquake (M_s = 6.6, M_w = 7.5, M_t = 7.8) [*Satake and*

Tanioka, 1999]. *Bourgeois et al*. [1999] find that the 1996 event is similar to the 1960 Peru event analyzed by *Pelayo and Wiens* [1990], with these two tsunami earthquakes being the only large subduction zone earthquakes in northern Peru since 1619, in what is inferred to be a subduction zone with a large component of aseismic convergence. The event occurred where the Mendaña Fracture zone is being subducted under the Peru margin (fig. 15.2). The seismic observations for this event were modeled by *Ihmlé et al*. [1998] and tsunami data were modeled by *Heinrich et al*. [1998] using the seismic slip model as a constraint. A 40-km-wide, 110-km-long fault model was used in the seismic modeling. The event ruptured bilaterally, updip of the epicenter with rupture velocity varying from 1.0 to 2.0 km/s and a total rupture duration of ~50 s. This is a relatively long duration for the moment magnitude, but not dramatically so, as for most of the events discussed above [e.g., *Polet and Kanamori*, 2000]. *Heinrich et al*. [1998] adopted this slip model to predict run-up heights and tide-gauge recordings along the Peruvian coast using a finite difference method for long wave equations. They found that a rigidity of 20 GPa reconciles the seismic and tsunami source models. Tsunami modeling by *Bourgeois et al*. [1999] using a 60-km-wide fault that is 120 km long with 4-m slip suggests a rigidity of 7.5 GPa. *Satake and Tanioka* [1999] modeled the tide-gauge records using either 40- or 80-km-wide faults extending up to the trench with slip of 4.5 and 2.2 m, respectively. Using a low rigidity of 10 GPa allows these slip models to be consistent with the seismic moment magnitude.

The tsunami earthquakes discussed above have common characteristics of shallow dipping thrust motion at shallow depths in material with very low rigidity of 5–10 GPa [*Satake and Tanioka*, 1999; *Synolakis et al*., 1997]. Figure 15.2 summarizes the narrow rupture zones at shallow depths favored for the 1896, 1946, 1992, and 1996 events [*Satake and Tanioka*, 1999]. All of these events are documented to have relatively long source process times, and in some cases, directly measured low rupture velocities. Figure 15.3 shows a schematic suggesting the distinct nature of rupture at very shallow depth in low rigidity material around the megathrust and resulting enhanced seafloor uplift documented for several of the large tsunami earthquakes. Note that an accretionary prism need not be present for this to occur, as in the case of the 1992 Nicaragua event, as long as sediments modify the frictional properties of the shallow portion of the megathrust.

There have been several other events in the broadband seismic data era that have generated unusually large tsunamis by other mechanisms. The 1992 Flores Islands (M_w 7.9) back-arc thrusting earthquake did not have slow rupture [e.g., *Imamura and Kikuchi*, 1994; *Beckers and Lay*, 1995; *Polet and Kanamori*, 2000], and most of the local tsunami is attributable to the seismic slip model, except for a 26.2-m run-up at Riangaroko, which is attributed to a local landslide effect by *Imamura et al*. [1995], *Tsuji et al*. [1995b], and *Hidayat et al*. [1995]. The small tsunami generated by the 1989 Loma Prieta earthquake was attributed to slumping in the Monterey Bay by *Ma et al*. [1991]. The 17 July 1998

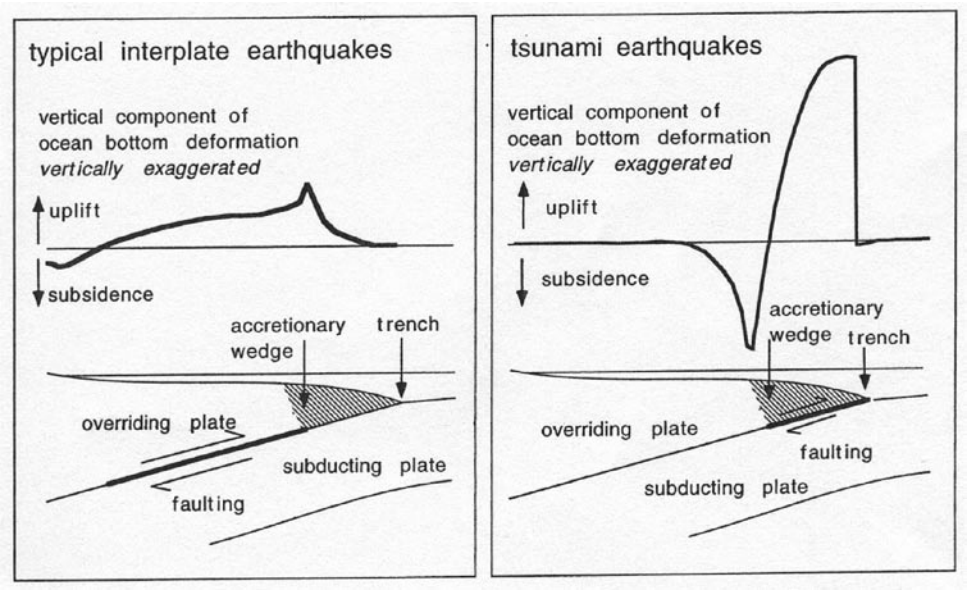

Figure 15.3 Schematic of slip at varying depth on the megathrust and resulting surface (ocean bottom) vertical displacement. Large slip at very shallow depth in low rigidity sediments causes large ocean bottom displacement relative to comparable seismic moment events with less slip in higher rigidity material at greater depth along the megathrust. This accounts for the strong tsunami excitation of some tsunami events; in some places, there is no accretionary wedge, and sediments subducted along the megathrust may play the same role. [From *Satake and Tanioka*, 1999].

Papua New Guinea (M_w 7.0) event produced a maximum tsunami run-up of 10–15 m on the coast in the vicinity of Sissano Lagoon. The seismic magnitudes for this event do not characterize it as having a particularly long rupture process or slow rupture velocity [e.g., *Newman and Okal*, 1998b; *Polet and Kanamori*, 2000]. Tsunami generation for this event is controversial, but it appears that this event is at least not a conventional interplate thrusting tsunami earthquake [*Geist* 1998, 2000; *Kawata et al*., 1999; *Matsuyama et al*., 1999; *Tanioka*, 1999; *Tappin et al*., 1999; *Synolakis et al*., 2002]. It is unclear whether the seismic models are able to account for the local tsunami run-up. *Kikuchi et al*. [1999] and *Tanioka* [1999] favor a steeply dipping fault plane rather than a shallowly dipping thrust plane as both the seismic and teleseismic tsunami source, although *Satake and Tanioka* [2003] suggest a combination of low angle faulting and a submarine landslide as the most likely source.

The 2 June 1994 East Java underthrusting earthquake (M_w 7.9) occurred in a region normally characterized as weakly seismically coupled. It produced local tsunami run ups that ranged from 1 to 14 m [*Tsuji et al*., 1995a], and *New-*

man and Okal [1998a] and *Polet and Kanamori* [2000] suggest that this event has low energy release, slow rupture, and location near the trench, which are consistent with it being a tsunami earthquake. *Abercrombie et al*. [2001] studied the seismic waves, finding a solution with shallow interplate thrusting ~12–20 km depth with an initial weak updip radiation over ~12 s. They found no evidence for anomalously slow, shallow slip, although it is notable that all of the larger aftershocks of this event involve normal faulting rather than thrusting. It was proposed that rupture of a seamount surrounded by stably sliding interface explains this event. The stress drop was estimated as 0.3~3 MPa, a low value comparable to estimates for the 1992 Nicaragua event, but the event was deemed to be different from typical tsunami events. *Tanioka and Satake* [1996b] model the tsunami using a shallow slip event near the trench, constraining the model by the seismic moment and using a rigidity of 40 GPa. This model underpredicts the tsunami by 30–50%, even allowing for horizontal movement of the ocean bottom, which enhances tsunami excitation in this case. Use of lower rigidity or more accurate run-up model could account for this, but *Abercrombie et al*. [2001] argue that the tsunami arrival times rule out a slip model as far seaward as the trench. *Polet and Thio* [2003] suggest slow particle velocity rather than slow rupture velocity might account for the weak short period radiation from the Java event relative to that for nearby aftershocks.

Large Events Deeper on the Megathrust Triggering Shallow Slip

The occurrence of significant seismic slip on the shallow portion of the megathrust, in some cases extending right up to the trench or to the margin of any sedimentary wedge, raises the question of whether this region fails during the rupture of great events at larger depth in the megathrust [*Geist*, 1998]. Inferences of earthquake rupture zones from aftershock distributions may be misleading, as in the case of the 1992 Nicaragua event, so it would seem plausible, and even likely, that during a large interplate rupture, slip may extend into the shallow megathrust where few, if any, aftershocks occur. Combined assessments of seismic, geodetic, and tsunami observations for great megathrust earthquakes have actually revealed that this is sometimes the case. *Hirata et al*. [2003] show that slip extended to shallow depth along a limited portion of the 1952 Tokachi-Oki earthquake, with rupture toward the southwest possibly being delimited by a subducted seamount. *Johnson and Satake* [1999] found that there was minor slip at shallow depth along a portion of the 1952 Kamchtaka rupture zone. *Satake* [1993] and *Tanioka and Satake* [2001a, 2001b] demonstrated that significant slip occurred at shallow depths along the Nankai region in the 1994 Tonankai and 1946 Nankai events. *Ichinose et al*. [2003] also find very shallow slip near the trench along the Kii peninsula for the 1994 Tonankai earthquake. *Johnson and Satake* [1996] estimated 1–3 m of slip along the shallow portion of the 1965 Rat Island earthquake. *Johnson et al*. [1996] found shallow

slip for the 1964 Alaska earthquake as well. The 9 October 1995 (M_w 8) Colima-Jalisco earthquake ruptured to shallow depths near the trench [*Mendoza and Hartzell*, 1999; *Pacheco et al*., 1997]. *Polet and Kanamori* [2000] note that some large events near Guerrero and Oaxaca, Mexico, have centroid locations displaced toward the trench as well. The occurrence of shallow slip may well have been more common in earlier events but simply was not recognized in the seismic data.

For some events it appears that slow slip on the updip portion of the megathrust precedes the mainshock at greater depth. This occurred for the 1968 Tokachi Oki earthquake [*Schwartz and Ruff*, 1985; *Satake*, 1989], for which a 30-s duration of low energy release preceded the mainshock, and for the 28 December 1994 Sanriku-oki earthquake (M_w 7.7), which initiated with a 20-s updip precursory slip followed by downdip rupture propagation [e.g., *Sato et al*., 1996; *Hartog and Schwartz*, 1996; *Tanioka et al*., 1996]. *Nakayama and Takeo* [1997] demonstrate that the precursory slip had a lower rupture velocity than the deeper primary slip. GPS observations revealed large aseismic afterslip following this event on both short term [*Heki and Tamura*, 1997] and long term [*Heki et al*., 1997], equaling the seismic moment of the mainshock, but with a time constant of over a year and with slip possibly overlapping the coseismic slip zone. Subsequent inversions of the GPS data indicate that postseismic slip occurred both updip and downdip of the coseismic slip, without significant spatial overlap with the co-seismic rupture area [*Uchida et al*., 2003; *Yagi et al*., 2003]. The aftershocks of the event extend far seaward of the main slip zone [e.g., *Matsuzawa et al*., 1995; *Hino et al*., 1996], overlapping the updip portion of the 1968 Tokachi-oki rupture zone. *Kawasaki et al*. [1995] found geodetic evidence for a very slow slip event in 1992 with a time constant of ~1 day to the south of this event. *Seno* [2002] summarizes the mainshock asperity zones and updip aftershock zones for the 1994, 1992, and 1989 events in this region, all of which have shallow aftershock zones overlapping the region of the 1896 tsunami event.

Moderate Size Earthquakes on the Shallow Megathrust

The unusual attributes of tsunami events and their destructive effects have focused attention on very large shallow megathrust earthquakes. While it is possible that these events have some uniqueness associated with their large slip and large total seismic moment, the interpretation of unusual frictional or mechanical properties at the source raises the question of whether smaller events rupturing the same area as a tsunami event have anomalous rupture properties, such as unusually low stress drop, slow rupture velocity, or slow particle velocities. This can be addressed by systematic analysis of moderate size earthquakes that are large enough to be well-recorded teleseismically,

which simplifies the analysis of the rupture process. In a series of papers, *Bilek and Lay* [1998, 1999a, 1999b, 2000] address this topic using data for 417 megathrust events. They find that after earthquake source time functions (determined by removing propagation effects from teleseismic *P* waves) are scaled to eliminate predictable differences due to total seismic moment, there is a systematic occurrence of unusually broad source time functions in the upper 10–15 km of many circum-Pacific megathrusts (fig. 15.4). Comparisons of moment-scaled source durations of these moderate size earthquakes with moment-scaled duration estimates from the known tsunami earthquakes suggests similar behavior (fig. 15.5), indicating that the frictional properties are not dependent on earthquake size. In addition, the general shape of the time functions for the shallow earthquakes is similar to time functions for several of the tsunami earthquakes [*Bilek and Lay*, 2002], with long tails of moment release and several subevents. Efforts to detect any correlation of the depth pattern in individual subduction zones with macroscopic attributes of each region (age of plate, bathymetric structures, etc.) have not yielded any strong correlations [*Bilek*, 2001].

The anomalously long source durations for the moderate size events cannot be unambiguously associated with slow rupture velocities, given that

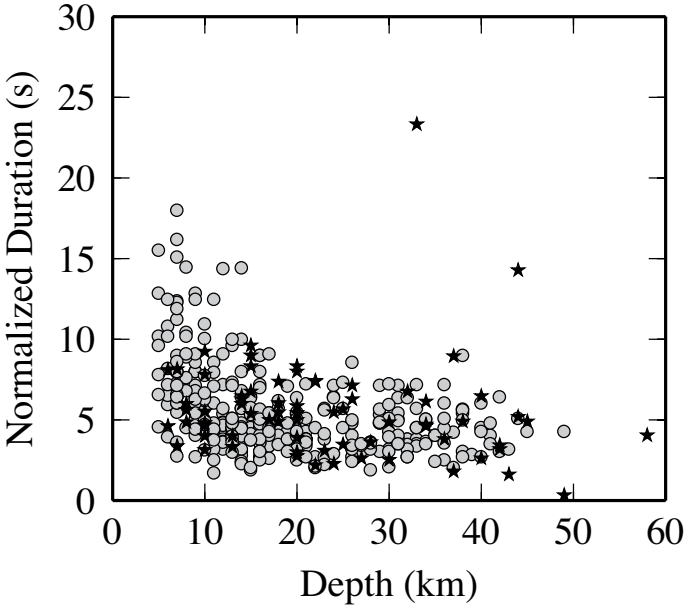

Figure 15.4 Earthquake rupture durations as a function of source depth for circum-Pacific subduction zone thrust events. The events are scaled to be normalized to M_w = 6.0. The circles are from the studies of *Bilek and Lay* [1999b, 2000] and *Bilek et al.* [2004], while the stars are from *Tanioka and Ruff* [1997] and updates in the University of Michigan source time function catalog.

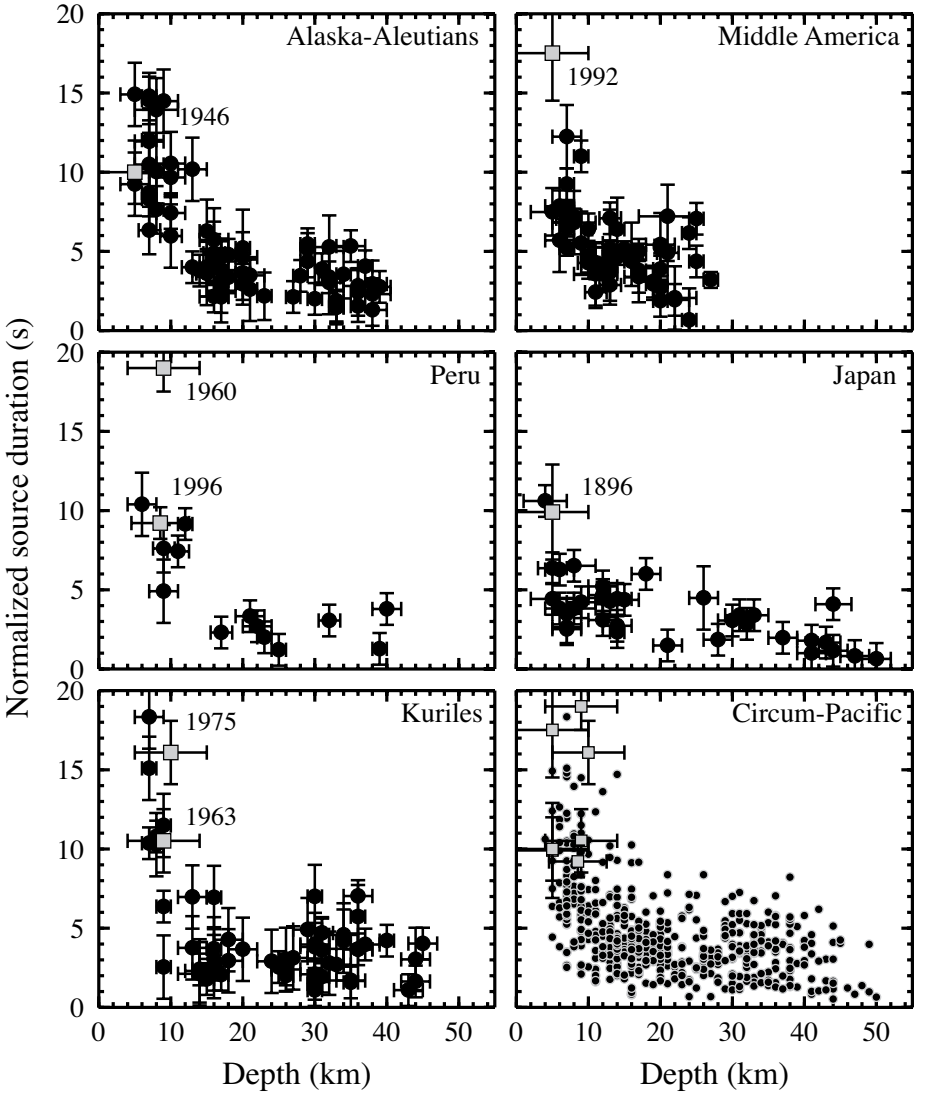

Figure 15.5 Earthquake rupture durations versus source depth for individual regions for the data from *Bilek and Lay* [1999b, 2000] and *Bilek et al.* [2004] along with moment-scaled source durations from large tsunami earthquakes in each of the five separate regions. All data are combined together at the lower right. Note that the tsunami events generally fall on or along the trend defined by the shallow events of intermediate size. [From *Bilek and Lay*, 2002].

point-source models were used to determine the source-time functions and no spatial finiteness is resolved. This leads to a complete trade-off between end-member models of events with low rupture velocity but normal (scaled) rupture area, or low stress drop events with normal (scaled) slip, but anomalously

large rupture area [e.g., *Bilek and Lay*, 1999b, 2000]. If it is assumed that rupture velocity is anomalously low (as demonstrated unambiguously to be the case for the 1992 Nicaragua event) and that rigidity is low, giving low shear velocity at the source and corresponding low rupture velocity, the source durations can be used to infer source rigidity variations as a function of depth (fig. 15.6a). Alternatively, one can map the durations into fault areas (assuming a given "normal" shear velocity), and then static stress drop variations as a function of depth can be estimated (fig. 15.6b). While it is likely that rupture velocity variations and stress drop variations are actually coupled, the data suggest an overall pattern of depth-dependent variations of rigidity and/or stress drop across the upper 10 km of the seismogenic zone. There is some indication of depth dependence of the ratio of seismic energy, *Es*, to seismic moment [*Bilek et al*., 2004] for individual regions, and all of the lowest values of this ratio (including the values for large tsunami earthquakes) are for events in the upper 10 km of the seismogenic zone. If future finite-source modeling of some of the long duration events is able to reveal the actual rupture velocities involved, it would allow the trade-off between rupture velocity and stress drop to be resolved, which would be a valuable contribution.

Additional studies have indicated anomalous rupture properties for moderate size earthquakes in the shallow subduction zone environment. *Houston* [2001] uses the source time function catalog of *Tanioka and Ruff* [1997] to examine variations in the shape and duration of time functions for a variety of tectonic settings. For a modest number (69) of megathrust events, she finds a general decrease in duration of about a factor of 1.5 from the shallowest (5–10 km) depth earthquakes to events at 30–40 km; a trend somewhat less than that apparent in the much larger data set of *Bilek and Lay* [2000]. Some differences in duration estimates for specific events are pointed out by *Houston* [2001], but she fails to note that these are associated with differences in depth estimates in most cases. *Ruff* [1999] uses the same catalog to explore dynamic stress drop variations along subduction zone megathrusts. In particular, *Ruff* [1999] highlights several earthquakes along the Oaxaca segment of the Mexican subduction zone that have significantly lower stress drops at the updip edge than earthquakes occurring at the downdip edge of seismicity. Other studies support a systematic depth variation in earthquake rupture properties along the Mexican subduction zone. *Shapiro et al*. [1998] and *Iglesias et al*. [2003] identify several near-trench shallow earthquakes that have low peak accelerations and are depleted in high-frequency radiation, similar to the depleted high-frequency radiation for tsunami earthquakes.

Okal and Newman [2001] use historical data to examine possible rupture anomalies for moderate and large earthquakes in regions of known tsunami earthquake occurrence, specifically Central America, Java, and Peru. They do not find a significant correlation between their slowness parameter (used to discriminate tsunami earthquakes) and depth, although they do question the values used for the historical earthquake depths. They do find regional

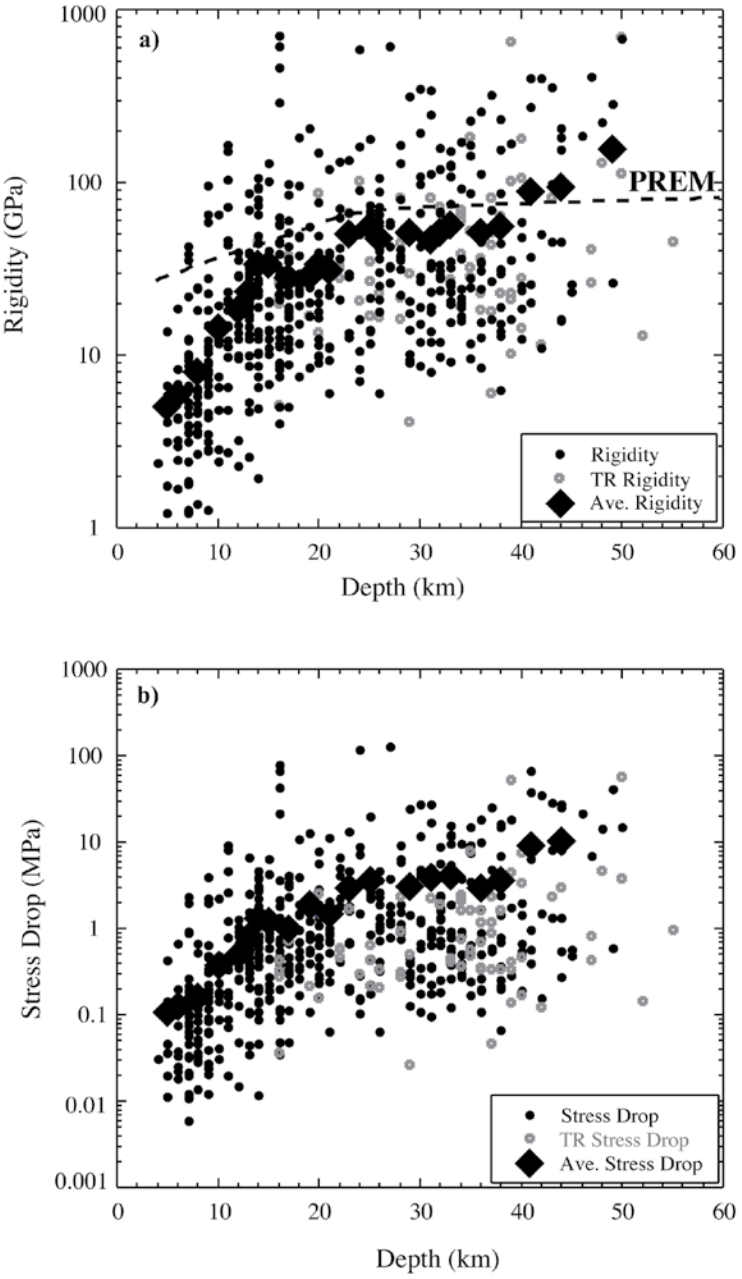

Figure 15.6 Estimates of source region rigidity (under assumption of constant stress drop) and source static stress drop (under the assumption of constant rupture velocity) for the source duration data of figure 15.4, plotted as functions of source depth. Open circles indicate data from *Tanioka and Ruff* [1997] and the solid circles are from the studies of *Bilek and Lay* [1999b, 2000] and *Bilek et al.* [2004]. Solid diamonds indicate mean values in depth bins. The values of rigidity from model PREM [*Dziewonski and Anderson*, 1981] are shown for reference.

correlations in that other slow earthquakes may have occurred in the regions of the 1992 Nicaragua and the 1960 and 1996 Peru tsunami earthquakes, and they suggest a local control on source slowness. The inclusion of events off the megathrust makes it difficult to assess this work.

The many observations of earthquake duration, stress drop, and source slowness variations along the shallow subduction megathrust suggest depth dependence of earthquake rupture process, even though it is unclear whether stress drop or rupture velocity increases with depth are dominant. This trend is similar to that which can be inferred on the basis of large earthquakes alone, although it appears to be more gradational than bimodal, as might be inferred just given large events. The systematic behavior observed for moderate and large events underlies the strategies being pursued for rapid tsunami hazard assessment [e.g., *Schindele et al*., 1995; *Newman and Okal*, 1998a].

Small Earthquakes on the Shallow Megathrust

Given the trends in large and moderate size earthquake rupture process with source depth, it is obviously important to examine yet smaller events to assess whether there is a scale dependence. Determining rupture characteristics for smaller earthquakes is actually a harder problem due to a lack of good quality data for most subduction zones. As the small event seismicity in the shallow megathrust is usually far offshore, adequate recording of the small earthquake signals usually requires ocean bottom seismometer (OBS) arrays.

Some early work on small magnitude earthquakes does suggest the possibility of anomalous behavior of the shallowest events. *Fukao and Kanjo* [1980] note a near-trench zone of shallow earthquakes extending along most of northern Japan that appear to generate low to very low frequency radiation. Their study of over 600 shallow earthquakes shows a distinct change in the frequency content of the earthquakes, with many high-frequency events occurring close to shore and presumably deeper along the megathrust. Examination of seismicity in the Kamchatka subduction zone suggests a gradient in source properties with depth, as the earthquakes located downdip from the trench radiate more high-frequency energy than those earthquakes occurring near the trench [*Zobin*, 1999].

OBS networks have been placed near several subduction zone margins in recent years, providing high-quality records for microseismicity in the megathrust zone. Earthquake distributions in northern Japan shows very little activity at the shallowest subduction zone depths beneath the margin wedge, with most activity occurring at depths of ~15 km even near the 1896 tsunami earthquake zone, which appears to have ruptured at shallow depth [*Nishizawa et al*., 1990; *Umino et al*., 1995; *Hino et al*., 1996; *Takahashi et al*., 2000]. Earthquake clustering in the shallow megathrust off Japan is common, suggesting lateral variations in the properties along the trench strike. To the south, around the

Nankai Trough, seismicity levels are very low; however, using an OBS network, *Obana et al*. [2003] note some plate interface microseismicity that suggests an updip limit offshore Cape Muroto, consistent with the 150° isotherm computed in regional thermal models. Rupture properties of the small events along Japan have not been systematically determined.

Several examinations of small earthquakes off Sanriku, Japan, suggest repeating earthquakes at small asperities. *Matsuzawa et al*. [2002] and *Igarashi et al*. [2003] find several clusters of microseismicity that are not collocated with regions of large moment release in previous earthquakes nor in areas identified as strongly coupled, and they estimate asperity size on the order of 0.1–1 km. These observations are used to describe a model for the NE Japan subduction zone including large asperities near the trench to support large earthquake occurrence, with smaller, sparsely distributed asperities and adjacent stable sliding zones deeper on the plate boundary. These observations have more recently been used to estimate quasi-static slip at this boundary. Assuming that the small asperities on the fault break in a characteristic manner, the time interval between each small earthquake is governed by the amount of aseismic slip in the adjacent regions [*Uchida et al*., 2003]. By estimating the slip released in these small earthquakes, *Uchida et al*. [2003] find regions of quasi-static slip in both the shallow and deepest portion of the plate boundary.

A combination of land and offshore seismic networks has been deployed in other subduction zones as well. *Husen et al*. [1999] use land stations and OBHs to relocate aftershocks of the 1995 M_w = 8.0 Antofagasta underthrust earthquake, defining a minimum seismogenic depth of 29 km. The upper limit of seismicity in northern Costa Rica appears to be transitional along the Nicoya Peninsula, shallowing from 20 km in the north to 10 km in the southern portion of the peninsula [*Newman et al*., 2002]. *Newman et al*. [2002] suggest a thermal cause for this transition with colder subducting crust in the north and warmer underthrusting crust in the south. In central Costa Rica, near the Osa Peninsula, *DeShon et al*. [2003] suggest that disrupted subducting crust influences the limits of seismogenesis, with an updip edge at a depth of 10 km. At this time, most effort has been placed on accurate event locations and defining the seismogenic limits in these margins, and comparing the seismic distribution with geodetic inferences of slipping and locked regions. Additional work will be needed for systematic exploration of possible rupture velocity or stress drop variations in these microseismicity data sets.

Nature of Friction on the Shallow Megathrust

The preceding overview of seismic failure characteristics for the shallow megathrust environment reveals substantial complexity. It is possible for large strains and/or slip deficits to accumulate in the shallow megathrust environment, for deeper slip events to induce slip at shallow depths, for slow shal-

low slip to precede deeper thrust faulting, and for slip to occur in large earthquakes at very shallow depth with almost no small events rupturing the same region. Clearly, the frictional properties of this region are not simply governed by pressure or temperature variations alone, with it being likely that bathymetric structures, sediments, pore-water pressures, and strain rates all play roles in the seismic behavior.

Estimates of the temperatures near the updip limit beneath sedimentary wedges are around 100°–150°C [e.g., *Hyndman et al*., 1997; *Oleskevich et al*., 1999], corresponding to the temperatures at which smectite undergoes most of its transformation to illite/chlorite [e.g., *Pytte and Reynolds*, 1989] along with occurrence of other diagenetic to low-grade metamorphic and consolidation phenomena that can affect fluid pressures in the megathrust (fig. 15.7; some of these processes are discussed elsewhere in this volume). The progressive dehydration of smectite along with consolidation and lithification of the prism sediments have thus been proposed as important mechanisms in the change in frictional properties associated with the onset of faulting [e.g., *Vrolijk*, 1990; *Morrow et al*., 1992; *Moore and Saffer*, 2001]. Recent experimental work suggests that illite actually does not exhibit the velocity-weakening behavior necessary for seismic slip, making it unlikely that the smectite to illite transition is directly responsible for the updip limit of seismicity in subduction zones [*Saffer and Marone*, 2003]. Smectite itself may exhibit unstable sliding as well [*Saffer et al*., 2001]. Thus more work is needed in order to understand other possible mechanisms and their role in controlling the updip seismicity limit.

Shallow megathrust faulting is commonly associated with low rupture velocity, for both large and small events. This observation raises the question of whether there is any effect of rupture in proximity to the free surface that influences faulting. The mechanics of dip-slip rupture are likely to be influenced if rupture extends to the surface, where there will essentially be a zero stress intensity condition. This will skew the dip-directed slip distribution in the updip direction [e.g., *Dmowska and Kostrov*, 1973; *Tse and Rice*, 1986; *Rudnicki and Wu*, 1995], with the large water depth near the trench enhancing the potential energy for excitation of tsunami gravity waves, as noted by *Geist and Bilek* [2001]. Even if seismic slip ends at the seismic front, anelastic seaward shoving of the shallow sedimentary wedge could effectively extend rupture to the surface, as in the idea of *Tanioka and Seno* [2001].

In the absence of specific knowledge about materials controlling friction in the shallow megathrust, it is still possible to characterize the overall behavior. The transition from stable sliding to unstable sliding appears to involve an intermediate behavior of conditional stability [e.g., *Scholz*, 1990, 1998]. Conditionally stable materials will typically undergo steady aseismic sliding but may fail coseismically if loaded at high strain rate. Earthquakes only nucleate in unstable zones, with their slip propagating into conditionally stable zones if they involve a strong enough velocity jump [*Scholz*, 1998]. Variation of the stability regime with depth and laterally with varying state variables gives

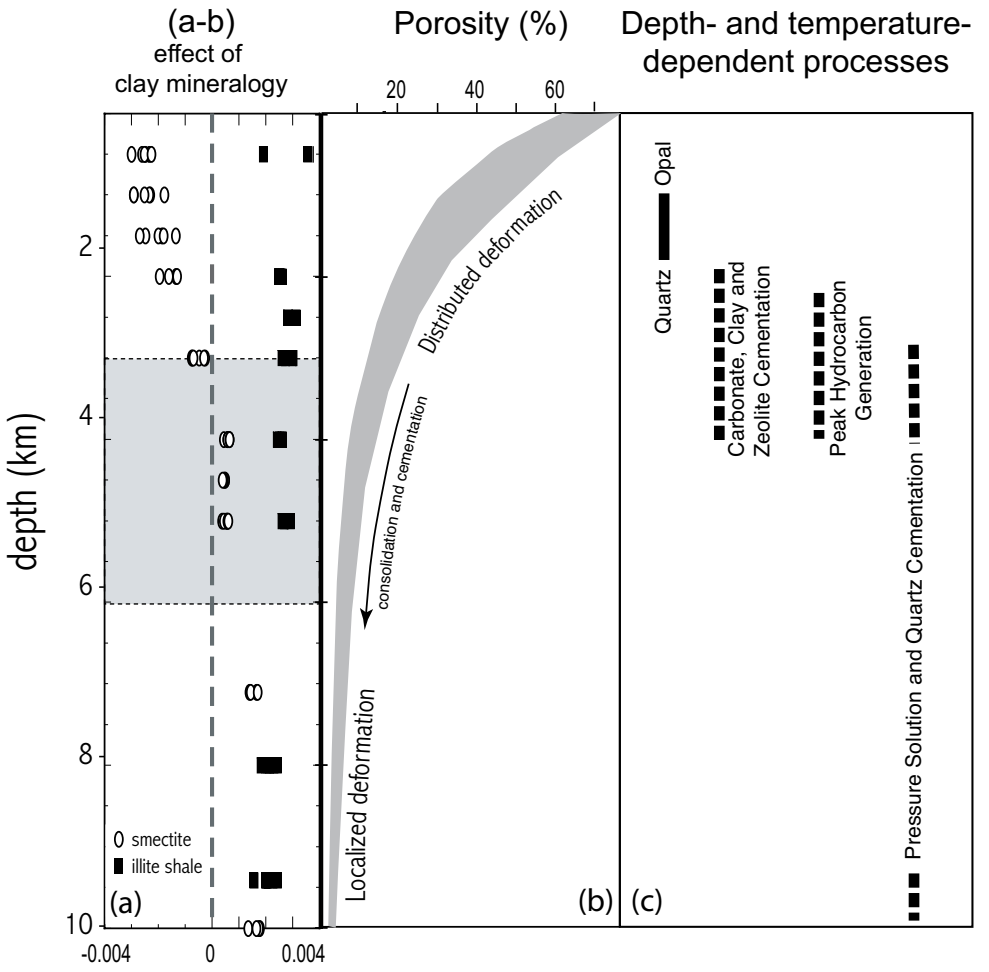

Figure 15.7 (a) Frictional velocity dependence for smectite (open circles) and illite shale (black squares) for up-step velocities of 20 mm/s, plotted with increasing depth assuming that effective stress increases by 10 MPa/km. Grey shaded region shows depth range for smectitie transformation. Dashed line denotes velocity-neutral behavior. Note that both materials exhibit only velocity-strengthening behavior at normal stresses above those corresponding to 4-km depth, and illite shale is velocity strengthening at all depths. (b) Porosity loss and associated transition from distributed deformation to localized slip hypothesized to explain updip limit of seismicity in accretionary wedges [e.g., *Moore and Saffer*, 2001]. (c) A suite of diagenetic and dehydration processes, including quartz phase transformation, cementation, fluid release from hydrous clays, and hydrocarbon generation and pressure. Courtesy of D. Saffer (2004)

rise to one-dimensional and two-dimensional characterizations of friction on the megathrust as shown in figure 15.8. *Scholz* [1998] presents a simple one-dimensional depth-varying model (fig. 15.8a), recognizing that there are going to be many lateral variations in properties. This suggests that the shallow

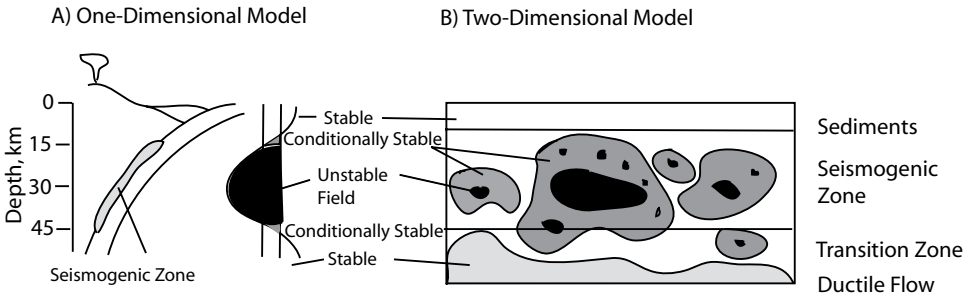

Figure 15.8 Conceptual models of frictional stability zones in subduction zones. A one-dimensional cartoon is shown on the left [modified from *Scholz*, 1999], emphasizing the transitions from stable sliding to unstable sliding involving zones of conditional stability at the updip and downdip edges of the seismogenic zone. A two-dimensional cartoon is shown on the right [modified from *Pacheco et al.*, 1993], emphasizing lateral variations along strike of the megathrust, with patches of unstable regime surrounded by conditionally stable and stable environments.

seismic zone just downdip from the aseismic front is likely to be conditionally stable. Shallow slip triggered by deeper strong faulting, as observed in many regions, would readily be accounted for. Tsunami earthquakes would involve slip within the conditionally stable regime in this case, presumably triggered by onset of slip at depth in the unstable regime. This is compatible with the updip rupture observed for several of the recent tsunami earthquakes such as the 1992 Nicaragua event [*Polet and Kanamori*, 2000]. *Pacheco et al*. [1993] envision the conditionally stable regime as surrounding patchy areas of unstable sliding regime throughout the seismogenic zone (fig. 15.8b). This is motivated by the need to accommodate large amounts of aseismic convergence in almost all regions. This is essentially a frictional stability regime perspective of the asperity model that has been used to discuss many earthquake ruptures.

A puzzle remains as to why very large strains/slip deficits accumulate in the conditionally stable zone to be released in large tsunami earthquakes. Given continuous convergence (with both slab-pull and ridge-push forces serving as driving forces), some type of buttressing of the conditional stability zone is needed to prevent slip from simply occurring at the plate motion rate. Downdip locked zones that are accumulating strain could allow some updip slip deficit to develop, with updip slip then occurring during large events at greater depth or possibly separately, triggered by minor slip of the downdip region. Localized regions of shallow frictional instability within the shallowest portion of the megathrust, associated with subducted bathymetric features such as seamounts or horst and graben structures (fig. 15.9) could also account for accumulation of strain [e.g., *Tanioka et al*., 1997; *Polet and Kanamori*, 2000].

It is also not evident why rupture in conditionally stable material will proceed at lower rupture velocity than in the unstable regime. The seismic and tsunami observations for large shallow tsunami events favor low source

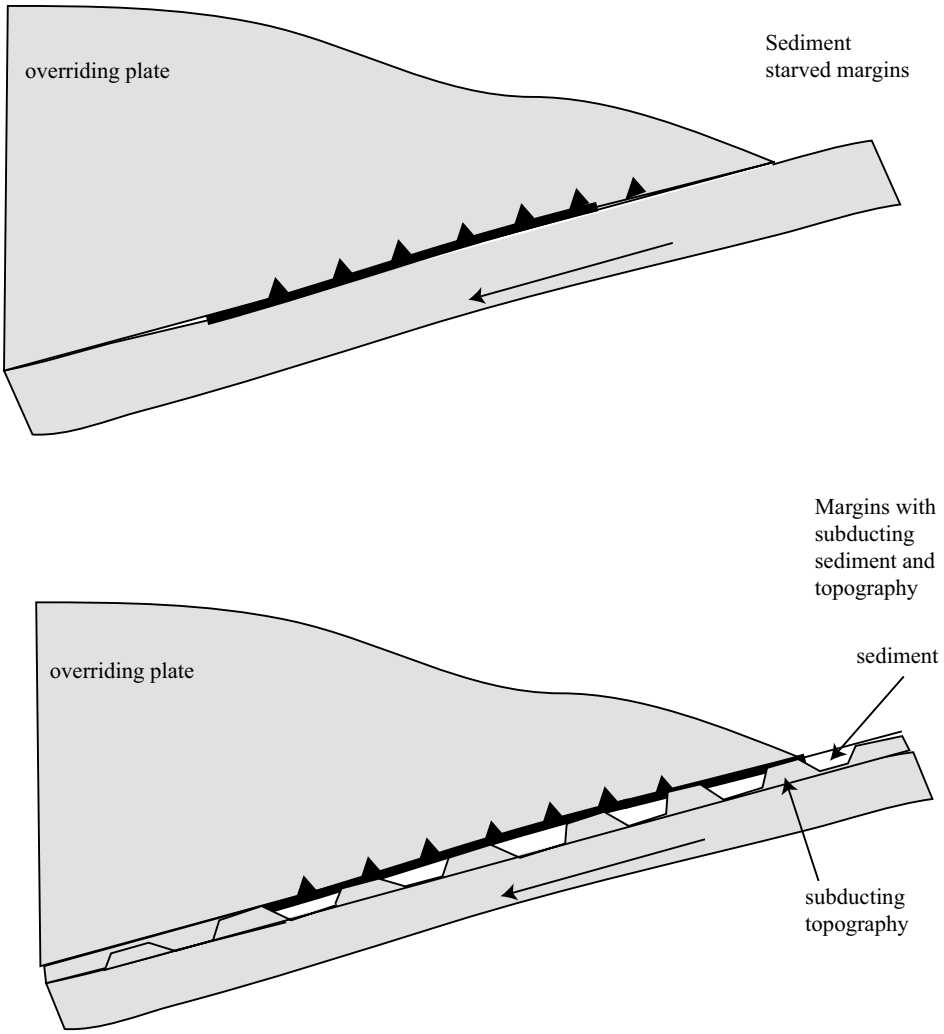

Figure 15.9 Bathymetric roughness in the form of seamounts or horst/graben structures, combined with sediment supply may have strong affects on the shallow megathrust environment. Sediment-starved margins may have no accretionary wedge, and if the bathymetry is relatively smooth, there may be uniform coupling of the interface with some sediments on the interface; rupture in these regions could extend to the trench. Regions with rough bathymetry and substantial sediment supply could have localized regions of unstable conditions within the conditionally stable zone.

zone rigidity, and this is compatible with the observations of long source process time and the few direct determinations of low rupture velocity. For smaller events the rupture durations are compatible with low source region rigidity as well, although low stress drop cannot be ruled out at this time, and

it is possible to lower the particle slip velocity rather than the rupture velocity to account for long processes times as well [e.g., *Polet and Thio*, 2003]. It is reasonable to associate the very low rigidities with the presence of sediments in the shallow megathrust, as these materials are expected to have low rigidities prior to dehydration and induration [e.g., *Bray and Karig*, 1985; *Schreve and Cloos*, 1986; *von Huene and Scholl*, 1991; *Kanamori and Kikuchi*, 1993; *Polet and Kanamori*, 2000]. The rigidity of sediments is dependent on sediment composition, water saturation, porosity, and pressure, with order of magnitude variations being observed in the laboratory [e.g., *Guerin and Goldberg*, 1996; *Mavko et al*., 1998]. The role of sediments may be twofold: such materials may tend to develop conditionally stable frictional behavior progressively with depth, and their low rigidities may control the overall strain release behavior by delimiting rupture velocity. Thus major aspects of anomalous faulting in the shallow megathrust may be explained. It remains difficult to assess subducted sediment budgets and to relate them to megathrust faulting [*Ruff*, 1989; *von Huene and Scholl*, 1991; *Rea and Ruff*, 1996; *Polet and Kanamori*, 2000]; however, the evidence for large slip in low rigidity material at shallow depth is strong.

Sediments may play the additional important role of controlling fluid content in the shallow megathrust. Many studies of shallow sedimentary conditions suggest that fluid pressures in the accretionary prism may be high and laterally variable [e.g., *Moore and Vrolijk*, 1992; *Tobin et al*., 1994; *Saffer and Bekins*, 1998; *Bekins and Screaton*, this volume; *Saffer*, this volume]. Presumably, heterogeneity in the permeability and pore pressures extends to variable depths in the megathrust, and *Pacheco et al*. [1993] invoke permeability variations as a primary state variable influencing heterogeneity in the frictional stability regime in their models. Fluids and weak properties of the fault zone are likely to play important roles in dynamic faulting processes [e.g., *Kanamori and Heaton*, 1999; *Brodsky and Kanamori*, 2001], which may provide an additional mechanism for distinctive rupture properties of very shallow megathrust events relative to deeper interplate thrusting. *Seno* [2002] suggests that increases of the area of zones of elevated fluid pressure may cause transition in the frictional sliding properties of subducted unconsolidated sediments. His idea is that transient changes in frictional stability occur owing to sealing and pressure buildup of the pore fluids, reducing effective normal stress. If pore pressures approach 90% of the lithostatic normal stress and the tectonic stress is not large, smectite could enter the unstable frictional regime [*Saffer et al*., 2001]. In this perspective the updip rupture extent for larger interplate thrusts may be influenced by the fluid state of the accretionary contact, with rupture either terminating far from the trench or diverting into splay faults or with rupture extending toward the trench resulting in strong tsunami excitation. Fluctuations in fluid pressure may thus help to account for the lack of shallow slip in the conditionally stable zone for many large megathrust ruptures and for subsequent rupture of those zones in tsunami earthquakes.

Figure 15.10, adapted from *Bilek and Lay* [2002], summarizes the frictional attributes of the shallow megathrust in a simplified form. This should be viewed as a snapshot in a steadily converging system loaded by slab pull and ridge-push, with frictional interactions across the megathrust being responsible for variations in slip on the interface. When there are off-scraped sediments in an accretionary wedge, there will typically be a shallow zone of aseismic stable sliding, with slip keeping pace with the plate convergence. Even large slip events at shallow depth will not rupture through this region as it will serve as a strain energy sink, although anelastic plowing of the material may occur. As pressure and temperature increase, the shallow megathrust enters the conditionally stable regime, possibly with localized patches of unstable frictional zones associated with bathymetric features such as seamounts, horst/graben structures, and variations in sediment permeability and pore pressure. The conditionally stable regime is heterogeneous laterally, and large tsunami earthquakes may induce large slip in this region that varies along strike (as for the 1992 Nicaragua event). Failure may initiate at the downdip edge of this region, as for the 1946 Aleutian and 1992 Nicaraguan events, or it may initiate on a patch of unstable friction such as an asperity, as in the 1994 Java event. In other regions this zone may slip continuously and aseismically. At greater

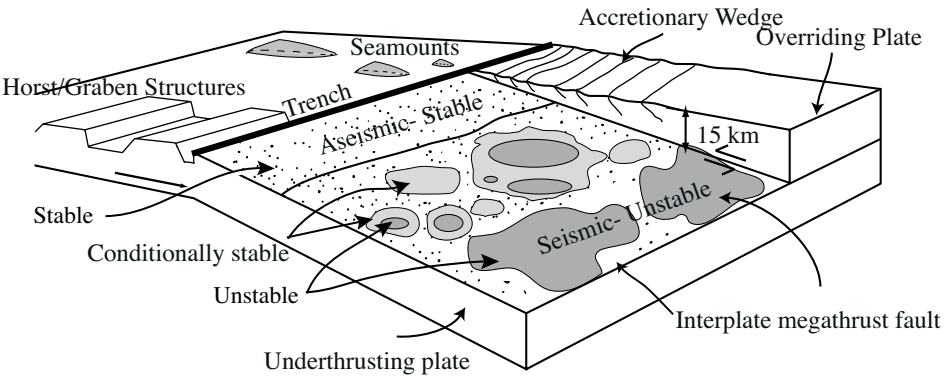

Figure 15.10 Cartoon of frictional properties on the shallow megathrust combining downdip and along-strike properties of the cartoons in figure 15.8. The shallowest region of the megathrust may be aseismic, with stable sliding if there are sediments accumulating in a sedimentary wedge of any significance. The upper 10 km or so of the megathrust seismogenic zone is dominated by stable and conditionally stable conditions, possibly with intermittent patches of unstable friction associated with variations in bathymetry, sediment, or fluid conditions. At greater depth the megathrust has an increasing percentage of unstable frictional conditions, although the percentage varies greatly from region to region. The unstable zones appear to be patchy, surrounded by conditionally stable or stable environments, giving rise to asperity type behavior of the large earthquake ruptures. Modified from *Bilek and Lay* [2002].

depth a larger percentage of the fault zone is in the unstable frictional regime, although there is still substantial aseismic slip in this domain in many subduction zones. Progressing from this cartoon notion will require improved constraints on the frictional properties of sediments, improved characterization of the fluid pressures at depth in the megathrust, and, ideally, in situ constraints on the detailed properties of the shallow megathrust.

Conclusions

The shallow portion of the megathrust in subduction zones exhibits complex seismogenic properties. While generally having low levels of seismicity, large slip events can occur at very shallow depth, and the resulting large ocean bottom displacement generates large tsunamis. The effective source region rigidity for these events is 2–4 times lower than typical hard rock values, suggesting that low rigidity sediments are on the fault plane. This is consistent with unusually long source process times and low rupture velocities documented for tsunami earthquakes. Slip in the tsunami earthquakes may extend updip of the aftershock zones and of the seismic front as defined by smaller events. Moderate size events on the megathrust tend to show some depth-dependent variations in rupture as well, with longer rupture durations found for events in the upper 10 km of the seismogenic zone. This is likely to reflect low rigidity of the shallow fault zone, increasing with depth due to sediment induration, fluid expulsion, and phase transformations in the sediments. The shallow megathrust appears to have a variable distribution of unstable and stable friction, with extensive zones of conditionally stable friction. Temporal fluctuations may occur due to variations in fluid properties, complicating the interpretation of this region.

Acknowledgments

We made extensive use of the Harvard CMT catalog. GMT software [*Wessel and Smith*, 1991] was used for some figure preparation. Kelin Wang provided a thorough review of the manuscript. All data from the IRIS Global Seismic Network were obtained from the IRIS DMS. This work was supported by NSF EAR 0125595. This is contribution number 474 of the Center for the Study of Imaging and Dynamics of the Earth, IGPP, University of California, Santa Cruz.

References

Abe, K. (1979), Size of great earthquakes of 1873–1974 inferred from tsunami data, *J. Geophys. Res., 84*, 1561–1568.

Abe, K. (1981), Physical size of tsunamigenic earthquakes of the northwestern Pacific, *Phys. Earth Planet Inter., 27*, 194–205.

Abercrombie, R. E., M. Antolik, K. Felzer, and G. Ekström (2001), The 1994 Java tsunami earthquake: Slip over a subducting seamount, *J. Geophys. Res., 106*, 6595–6607.

Beck, S., and L. Ruff (1989), Great earthquakes and subduction along the Peru trench, *Phys. Earth Planet. Int., 57*, 199–224.

Beckers, J., and T. Lay (1995), Very broadband seismic analysis of the 1992 Flores, Indonesia, earthquake (M_w = 7.9), *J. Geophys. Res., 100*, 18,179–18,193.

Bekins, B. A., and E. J. Screaton (2007), Pore pressure and fluid flow in the northern Barbados accretionary complex: A synthesis, this volume.

Bilek, S. L. (2001), Earthquake rupture processes in circum-Pacific subduction zones. Ph.D. thesis, 180 pp., Univ. Calif., Santa Cruz.

Bilek, S. L. (2007), Influence of subducting topography on earthquake rupture, this volume.

Bilek, S. L., and T. Lay (1998), Variation of interplate fault zone properties with depth in the Japan subduction zone, *Science, 281*, 1175–1178.

Bilek, S. L., and T. Lay (1999a), Comparison of depth dependent fault zone properties in the Japan trench and Middle America trench, *Pure Appl. Geophys., 154*, 433–456.

Bilek, S. L., and T. Lay (1999b), Rigidity variations with depth along interplate megathrust faults in subduction zones, *Nature, 400*, 443–446.

Bilek, S. L., and T. Lay (2000), Depth dependent rupture properties in circum-Pacific subduction zones, in *Geocomplexity and the Physics of Earthquakes*, *Geophys. Monogr. Ser.*, vol. 120, edited by J. B. Rundle, D. L. Turcotte, and W. Klein, pp. 165–186. AGU, Washington, D. C.

Bilek, S. L., and T. Lay (2002), Tsunami earthquakes possibly widespread manifestations of frictional conditional stability, *Geophys. Res. Lett., 2*(14), 1673, doi:10.1029/2002GL015215.

Bilek, S. L., T. Lay, and L. J. Ruff (2004), Radiated seismic energy and earthquake source duration variations from teleseismic source time functions for shallow subduction zone thrust earthquakes, *J. Geophys. Res., 109*, B09308, doi:10.1029/2004JB003039.

Bourgeois, J., C. Petroff, H. Yeh, V. Titov, C. E. Synolakis, B. Benson, J. Kuroiwa, J. Lander, and E. Norabuena (1999), Geologic setting, field survey and modeling of the Chimbote, northern Peru, tsunami of 21 February 1996, *Pure Appl. Geophys., 154*, 513–540.

Bray, C., and D. Karig (1985), Porosity of sediments in accretionary prisms and some implications for dewatering processes, *J. Geophys. Res., 90*, 768–778.

Brodsky, E. E., and H. Kanamori (2001), Elastohydrodynamic lubrication of faults, *J. Geophys. Res., 106*, 16,357–16,374.

Byrne, T., D. Davis, and L. Sykes (1988), Loci and maximum size of thrust earthquakes and the mechanics of the shallow region of subduction zones, *Tectonics, 7*, 833–857.

Choy, G., and J. Boatwright (1995), Global patterns of radiated seismic energy and apparent stress, *J. Geophys. Res., 100*, 18,205–18,228.

Cloos, M. (1992), Thrust-type subduction zone earthquakes and seamount asperities: A physical model for seismic rupture, *Geology, 20*(7), 601–604.

Cloos, M., and R. L. Shreve (1996), Shear-zone thickness and the seismicity of Chilean- and Marianas-type subduction zones, *Geology, 24*(2), 107–110.

Cummins, P. R., and Y. Kaneda (2000), Possible splay fault slip during the 1946 Nankai earthquake, *Geophys. Res. Lett., 27*, 2725–2728.

DeShon, H. R., S. Y. Schwartz, S. L. Bilek, L. M. Dorman, V. Gonzalez, J. M. Protti, E. R. Flueh, and T. H. Dixon (2003), Seismogenic zone structure of the southern Middle America trench, Costa Rica, *J. Geophys. Res., 108*(B10), 2491, doi:10.1029/ 2002JB002294.

Dmowska, R., and B. V. Kostrov (1973), A shearing crack in a semi-space under plane strain conditions, *Arch. Mech., 25*, 421–440.

Dziewonski, A., and D. L. Anderson (1981), Preliminary reference earth model, *Phys. Earth Planet. Int., 25*, 297–356.

Dziewonski, A. M., G. Ekström, and M. P. Salganik (1993), Centroid-moment tensor solutions for July-September 1992, *Phys. Earth Planet Int., 79*, 287–297.

Fukao, Y. (1979), Tsunami earthquakes and subduction processes near deep-sea trenches, *J. Geophys. Res., 84*, 2303–2314.

Fukao, Y., and K. Kanjo (1980), A zone of low-frequency earthquakes beneath the inner wall of the Japan Trench, *Tectonophysics, 67*, 153–162.

Geist, E. L. (1998), Local tsunamis and earthquake source parameters, *Adv. Geophys., 39*, 117–209.

Geist, E. L. (2000), Origin of the 17 July 1998 Papua New Guinea tsunami: Earthquake or landslide? *Seismol. Res. Lett., 71*, 344–350.

Geist, E. L., and S. Bilek (2001), Effect of depth-dependent shear modulus on tsunami generation along subduction zones, *Geophys. Res. Lett., 28*, 1315–1318.

Guerin, G., and D. Goldberg (1996), Acoustic and elastic properties of calcareous sediments across a siliceous diagenetic front on the eastern U.S. continental slope, *Geophys. Res. Lett., 23*, 2697–2700.

Gutscher, M.-A., and S. M. Peacock (2003), Thermal models of flat subduction and the rupture zone of great subduction earthquakes, *J. Geophys. Res., 108*(B1), 2009, doi:10.1029/2001JB000787.

Harlow, D. H., R. A. White, I. L. Cifuentes, and A. Aburto (1981), Quiet zone within a seismic gap near western Nicaragua: Possible location of a future large earthquake, *Science, 213*, 648–651.

Hartog, R., and S. Schwartz (1996), Directivity analysis of the December 28, 1994 Sanriku-oki earthquake (M_w = 7.7), Japan, *Geophys. Res. Lett., 23*, 2037–2040.

Hasegawa, H. S., and H. Kanamori (1987), Source mechanism of the magnitude 7.2 Grand Banks earthquake of November 1927: Double couple or submarine landslide? *Bull. Seismol. Soc. Am., 77*, 1984–2004.

Heinrich, P., F. Schindele, S. Guibourg, and P. F. Ihmlé (1998), Modeling of the February 1996 Peruvian tsunami, *Geophys. Res. Lett., 25*, 2687–2690.

Heki, K., and Y. Tamura (1997), Short term afterslip in the 1994 Sanriki-Haruka-Oki earthquake, *Geophys. Res. Lett., 24*, 3285–3288.

Heki, K., S. Miyazaki, and H. Tsuji (1997), Silent fault slip following an interplate thrust earthquake at the Japan trench, *Nature, 386*, 595–598.

Hidayat, D., J. S. Barker, and K. Satake (1995), Modeling the seismic source and tsunami generation of the December 12, 1992, Flores island, Indonesia, earthquake, *Pure Appl. Geophys., 144*, 537–554.

Hino, R., T. Kanazawa, and A. Hasegawa (1996), Interplate seismic activity near the northern Japan Trench deduced from ocean bottom and land-based seismic observations, *Phys. Earth Planet. Inter., 93*, 37–52.

Hirata, K., E. Geist, K. Satake, Y. Tanioka, and S. Yamaki (2003), Slip distribution of the 1952 Tokachi-Oki earthquake (*M* 8.1) along the Kuril Trench deduced from tsunami waveform inversion, *J. Geophys. Res., 108*(B4), 2196, doi:10.1029/2002JB001976.

Houston, H. (2001), Influence of depth, focal mechanism, and tectonic setting on the shape and duration of earthquake source time functions, *J. Geophys. Res., 106*, 11,137–11,150.

Husen, S., E. Kissling, E. Flueh, and G. Asch (1999), Accurate hypocentre determination in the seismogenic zone of the subducting Nazca Plate in northern Chile using a combined on-/offshore network, *Geophys. J. Int., 138*, 687–701.

Husen, S., E. Kissling, and R. Quintero (2002), Tomographic evidence for a subducted seamount beneath the Gulf of Nicoya, Costa Rica: The cause of the 1990 M_w = 7.0 Gulf of Nicoya earthquake, *Geophys. Res. Lett., 29*(8), 1238, doi:10.1029/2001GL014045.

Hyndman, R. D., and K. Wang (1993), Thermal constraints on the zone of major thrust earthquake failure: The Cascadia subduction zone, *J. Geophys. Res., 98*, 2039–2060.

Hyndman, R. D., K. Wang, and M. Yamano (1995), Thermal constraints on the seismogenic portion of the southwestern Japan subduction thrust, *J. Geophys. Res., 100*, 15,373–15,392.

Hyndman, R. D., M. Yamano, and D. A. Oleskevich (1997), The seismogenic zone of subduction thrust faults, *Island Arc, 6*, 244–260.

Ichinose, G. A., H.-K. Thio, P. G. Somerville, T. Sato, T., and T. Ishii (2003), Rupture process of the 1944 Tonankai earthquake (M_s 8.1) from the inversion of teleseismic and regional seismograms, *J. Geophys. Res. 108*(B10), 2497, doi:10.1029/2003JB002393.

Ide, S., F. Imamura, Y. Yoshida, and K. Abe (1993), Source characteristics of the Nicaraguan tsunami earthquake of September 2, 1992, *Geophys. Res. Lett., 20*, 863–866.

Igarashi, T., T. Matsuzawa, and A. Hasegawa (2003), Repeating earthquakes and interplate aseismic slip in the northeastern Japan subduction zone, *J. Geophys. Res., 108*(B5), 2249, doi:10.1029/2002JB001920.

Iglesias, A., S. K. Singh, J. F. Pacheco, L. Alcántara, M. Ortiz, and M. Ordaz (2003), Near-trench Mexican earthquakes have anomalously low peak accelerations, *Bull. Seismol. Soc. Am., 93*, 953–959.

Ihmlé, P. F. (1994), Teleseismic study of rupture processes with long duration, Ph.D. thesis, Mass. Inst. of Technol., Cambridge.

Ihmlé, P. F. (1996a), Frequency-dependent relocation of the 1992 Nicaragua slow earthquake: An empirical Green's function approach, *Geophys. J. Int., 127*, 75–85.

Ihmlé, P. F. (1996b), Monte Carlo slip inversion in the frequency domain: Application to the 1992 Nicaragua slow earthquake, *Geophys. Res. Lett., 23*, 913–916.

Ihmlé, P. F., J.-M. Gomez, P. Heinrich, and S. Guibourg (1998), The 1996 Peru tsunamigenic earthquake: Broadband source process, *Geophys. Res. Lett., 25*, 2691–2694.

Imamura, F. M., and Kikuchi (1994), Moment release of the 1992 Flores Island earthquake inferred from tsunami and teleseismic data, *Sci. Tsunami Hazards, 12*, 67–76.

Imamura, F., E. Gica, T. Takahashi, T., and N. Shuto (1995), Numerical simulation of the 1992 Flores tsunami: Interpretation of tsunami phenomena in northeastern Flores Island and damage at Babi Island, *Pure Appl. Geophys., 144*, 555–568.

Imamura, F., N. Shuto, S. Ide, Y. Yoshida, and K. Abe (1993), Estimate of the tsunami source of the 1992 Nicaraguan earthquake from tsunami data, *Geophys. Res. Lett., 20*, 1515–1518.

Jarrard, R. (1986), Relation among subduction parameters, *Rev. Geophys., 24*, 217–284.

Johnson, J. M., and K. Satake (1996), The 1965 Rat Islands earthquake: A critical comparison of seismic and tsunami wave inversions, *Bull. Seismol. Soc. Am., 86*, 1229–1237.

Johnson, J. M., and K. Satake (1997), Estimation of seismic moment and slip distribution of the April 1, 1946, Aleutian tsunami earthquake, *J. Geophys. Res., 102*, 11,765–11,779.

Johnson, J. M., and K. Satake (1999), Asperity distribution of the 1952 great Kamchatka earthquake and its relation to future earthquake potential in Kamchatka, *Pure Appl. Geophys., 154*, 541–553.

Johnson, J. M., K. Satake, S. R. Holdahl, and J. Sauber (1996), The 1964 Prince William Sound earthquake: Joint inversion of tsunami and geodetic data, *J. Geophys. Res., 101*, 523–532.

Kanamori, H. (1972), Mechanism of tsunami earthquakes, *Phys. Earth Planet. Int., 6*, 246–259.

Kanamori, H. (1977), Seismic and aseismic slip along subduction zones and their tectonic implications, in *Island Arcs, Deep Sea Trenches and Back-Arc Basins, Maurice Ewing Series,* vol. 1, edited by M. Talwani and W. C. Pittman, pp. 163–174. AGU, Washington, D. C.

Kanamori, H. (1985), Non double-couple seismic source, in XXIIIrd General Assembly, vol. 2, p. 425, Abstract S7-56, Int. Assoc. of Seismol. and Phys. of Earth Inter., Tokyo, Japan.

Kanamori, H. (1986), Rupture process of subduction-zone earthquakes, *Annu. Rev. Earth Planet. Sci., 14*, 293–322.

Kanamori, H. (1993), W phase, *Geophys Res. Lett., 20*, 1691–1694.

Kanamori, H., and T. H. Heaton (1999), Microscopic and macroscopic physics of earthquakes, in *Geocomplexity and the Physics of Earthquakes, Geophys. Monogr. Ser.,* vol. 120, edited by J. B. Rundle, D. L. Turcotte, and W. Klein, pp. 147–163, AGU, Washington, D. C.

Kanamori, H., and M. Kikuchi (1993), The 1992 Nicaragua earthquake: A slow tsunami earthquake associated with subducted sediments, *Nature, 361*, 714–716.

Kawasaki, I., Y. Asai, Y. Tamura, T. Sagiya, N. Mikami, Y. Okada, M. Sakata, and M. Kasahara (1995), The 1992 Sanriku-Oki, Japan, ultra-slow earthquake, *J. Phys. Earth, 43*, 105–116.

Kawata, Y., B. Benson, J. Borrero, H. Davies, W. de Lange, F. Imamura, H. Letz, J. Nott, and C. Synolakis (1999), Tsunami in Papua New Guinea was as intense as first thought, *Eos Trans. AGU, 80*, 101–105.

Kelleher, J., and W. McCann (1976), Buoyant zones, great earthquakes and unstable boundaries of subduction, *J. Geophys. Res., 81*, 4885–4896.

Kikuchi, M., and Y. Fukao (1987), Inversion of long-period P waves from great earthquakes along subduction zones, *Tectonophysics, 144*, 231–247.

Kikuchi, M., and H. Kanamori (1995), Source characteristics of the 1992 Nicaragua tsunami earthquake inferred from teleseismic body waves, *Pure Appl. Geophys., 144*, 441–453.

Kikuchi, M., Y. Yamanaka, K. Abe, and Y. Morita (1999), Source rupture process of the Papua New Guinea earthquake of 17 July 1998 inferred from teleseismic body waves, *Earth Planets Space, 51*, 1319–1324.

Kodaira, S., N. Takahashi, A. Nakanishi, S. Miura, and Y. Kaneda (2000), Subducted seamount imaged in the rupture zone of the 1946 Nankaido earthquake, *Science, 289*, 104–106.

Lay, T., and H. Kanamori (1981), An asperity model of great earthquake sequences, in *Earthquake Prediction: An International Review, Maurice Ewing Ser.*, vol. 4., edited by D. Simpson and P. Richards, pp. 579–592. AGU, Washington, D. C.

Lay, T., H. Kanamori, and L. Ruff (1982), The asperity model and the nature of large subduction zone earthquakes, *Earthquake Pred. Res., 1*, 3–71.

Ma, K.-F., K. Satake, and H. Kanamori (1991), The origins of the tsunami excited by the 1989 Loma Prieta earthquake--faulting or slumping, *Geophys. Res. Lett., 18*, 637–640.

Marone, C., and D. Saffer (2007), Fault friction and the upper transition from seismic to aseismic faulting, this volume.

Marone, C., and C. H. Scholz (1988), The depth of seismic faulting and the upper transition from stable to unstable slip regimes, *Geophys. Res. Lett., 15*, 621–624.

Matsuyama, M., J. P. Walsh, and H. Yeh (1999), The effect of bathymetry on tsunami characteristics at Sissano Lagoon, Papua New Guinea, *Geophys. Res. Lett., 26*, 3513–3516.

Matsuzawa, T., T. Igarashi, and A. Hasegawa (2002), Characteristic small-earthquake sequence off Sanriku, northeastern Honshu, Japan, *Geophys. Res. Lett., 29*(11), 1543, doi:10.1029/2001GL014632.

Matsuzawa, T., N. Umino, A. Hasegawa, M. Kosuga, K. Tanaka, K., and M. Kasahara (1995), Aftershock activity of the 1994 far off Sanriku earthquake observed by a microearthquake observation network (in Japanese), Rep. 06306019, Sci. Res. Fund by the Minist. of Educ. Sci. and Culture of Japan.

Mavko, G., T. Mukerji, T., and J. Dvorkin (1998), *The Rock Physics Handbook: Tools for Seismic Analysis in Porous Media*, Cambridge Univ. Press, New York.

McCaffrey, R. (1993), On the role of the upper plate in great subduction zone earthquakes, *J. Geophys. Res., 98*, 11,953–11,966.

McCaffrey, R. (1997), Statistical significance of the seismic coupling coefficient, *Bull. Seismol. Soc. Am., 87*, 1069–1073.

Mendoza, C., and S. Hartzell (1999), Fault-slip distribution of the 1995 Colima-Jalisco, Mexico, earthquake, *Bull. Seismol. Soc. Am., 89*, 1338–1344.

Moore, J. C., and D. Saffer (2001), The updip limit of the seismogenic zone beneath the accretionary prism of southwest Japan: An effect of diagenetic to low-grade metamorphic processes and increasing effective stress, *Geology, 29*(2), 183–186.

Moore, J. C., and P. Vrolijk (1992), Fluids in accretionary prisms, *Rev. Geophys., 30*, 113–135.

Morrow, C. A., B. Radney, and J. Byerlee (1992), Frictional strength and the effective pressure law of montmorillonite and illite clays, in *Fault Mechanics and Transport Properties of Rocks*, edited by B. Evans, pp. 69–88, Elsevier, New York.

Nakayama, W., and M. Takeo (1997), Slip history of the 1994 Sanriku-Haruka-Oki, Japan earthquake deduced from strong-motion data, *Bull. Seismol. Soc. Am., 87*, 918–931.

Newman, A. V., and E. A. Okal (1998a), Teleseismic estimates of radiated seismic energy: The E/Mo discriminant for tsunami earthquakes, *J. Geophys. Res., 103*, 26, 885–26,898.

Newman, A. V., and E. A. Okal (1998b), Moderately slow character of the 17 July 1998 Sandaun earthquake as studied by teleseismic energy estimates, *Eos Trans. AGU*, 79, Fall Meet. Suppl., F564.

Newman, A. V., S. Y. Schwartz, V. Gonzalez, H. R. DeShon, J. M. Protti, and L. M. Dorman (2002), Along-strike variability in the seismogenic zone below Nicoya Peninsula, Costa Rica, *Geophys. Res. Lett., 29*(20), 1977, doi:10.1029/2002GL015409.

Nishizawa, A., T. Kono, A. Hasegawa, T. Hirasawa, T. Kanazawa, and T. Iwasaki (1990), Spatial distribution of earthquake off Sanriku, northeaster Japan, in 1989 determined by ocean-bottom and land-based observation, *J. Phys. Earth, 38*, 347–360.

Obana, K., S. Kodaira, Y. Kaneda, K. Mochizuki, M. Shinohara, and K. Suyehiro (2003), Micro-seismicity at the seaward updip limit of the western Nankai Trough seismogenic zone, *J. Geophys. Res., 108*(B10), 2459, doi:10.1029/2002JB002370.

Okal, E. A. (1988), Seismic parameters controlling far-field tsunami amplitudes: A review, *Nat. Hazards, 1*, 67–96.

Okal, E. A., and A. V. Newman (2001), Tsunami earthquakes: the quest for a regional signal, *Phys. Earth Planet. Inter., 124*, 45–70.

Oleskevich, D. A., R. D. Hyndman, and K. Wang (1999), The updip and downdip limits to great subduction earthquakes: Thermal and structural models of Cascadia, south Alaska, SW Japan, and Chile, *J. Geophys. Res., 104*, 14,965–14,991.

Pacheco, J. F., and L. R, Sykes (1992), Seismic moment catalog for large shallow earthquakes from 1900 to 1989, *Bull. Seismol. Soc., 82*, 1306–1349.

Pacheco, J. F., L. R. Sykes, and C. H. Scholz (1993), Nature of seismic coupling along simple plate boundaries of the subduction type, *J. Geophys. Res., 98*, 14,133–14,159.

Pacheco, J., et al. (1997), The October 9, 1995 Colima-Jalisco, Mexico earthquake (M_w 8): An aftershock study and a comparison of this earthquake with those of 1932, *Geophys. Res. Lett., 24*, 2223–2226.

Park, J. O., T. Tsuru, S. Kodaira, P. R. Cummins, and Y. Kaneda (2002), Splay fault branching along the Nankai subduction zone, *Science, 297*, 1157–1160.

Peacock, S. M., and R. D. Hyndman (1999), Hydrous minerals in the mantle wedge and the maximum depth of subduction thrust earthquakes, *Geophys. Res. Lett., 26*, 2517–2520.

Pelayo, A. M. (1990), Earthquake source parameter inversion using body and surface waves: Applications to tsunami earthquakes and Scotia Sea seismotectonics, Ph.D. thesis, Washington Univ., St. Louis, Mo.

Pelayo, A. M., and D. A. Wiens (1990), The November 20, 1960 Peru tsunami earthquake: Source mechanism of a slow earthquake, *Geophys. Res. Lett., 17*, 661–664.

Pelayo, A. M., and D. A. Wiens (1992), Tsunami earthquakes: Slow thrust-faulting events in the accretionary wedge, *J. Geophys. Res., 97*, 15,321–15,337.

Peterson, E., and T. Seno (1984), Factors affecting seismic moment release rates in subduction zones, *J. Geophys. Res., 89*, 10,233–10,248.

Piatanesi, A., S. Tinti, and I. Gavagni (1996), The slip distribution of the 1992 Nicaragua earthquake from tsunami run-up data, *Geophys. Res. Lett., 23*, 37–40.

Polet, J., and H. Kanamori (2000), Shallow subduction zone earthquakes and their tsunamigenic potential, *Geophys. J. Int., 142*, 684–702.

Polet, J., and H. K. Thio (2003), The 1994 Java tsunami earthquake and its "normal" aftershocks, *Geophys. Res. Lett., 30*(9), 1474, doi:10.1029/2002Gl016806.

Pytte, A M., and R. C. Reynolds (1989), The thermal transformation of smectite to illite, in *Thermal History of Sedimentary Basins: Methods and Case Histories*, edited by Naeser, N. D. and T. H. McCulloh, pp. 33–40, Springer, New York.

Rea, D., and L. J. Ruff (1996), Composition and mass flux of sediment entering the world's subduction zones: Implications for global sediment budgets, great earthquakes and volcanism, *Earth and Planet. Sci. Lett., 140*, 1–12.

Rudnicki, J. W., and M. Wu (1995), Mechanics of up-slip faulting in an elastic half-space, *J. Geophys. Res., 100*, 22,173–22,186.
Ruff, L. J. (1989), Do trench sediments affect great earthquake occurrence in subduction zones? *Pure Appl. Geophys., 129*, 263–282.
Ruff, L. J. (1992), Asperity distributions and large earthquake occurrence in subduction zones, *Tectonophysics, 211*, 61–83.
Ruff, L. J. (1999), Dynamic stress drop of recent earthquakes: Variations within subduction zones, *Pure Appl. Geophys., 154*, 409–431.
Ruff, L. J., and H. Kanamori (1980), Seismicity and the subduction process, *Phys. Earth Planet. Inter., 23*, 240–252.
Ruff, L. J., and H. Kanamori (1983a), Seismic coupling and uncoupling at subduction zones, *Tectonophysics, 99*, 99–117.
Ruff, L. J., and H. Kanamori (1983b), The rupture process and asperity distribution of three great earthquakes from long period diffracted *P*-waves, *Phys. Earth Planet. Int., 31*, 202–230.
Ruff, L. J., and A. D. Miller (1994), Rupture process of large earthquakes in the northern Mexico subduction zone, *Pure Appl. Geophys., 142*, 101–171.
Saffer, D. (2007), Pore pressure within underthrust sediments in subduction zones, this volume.
Saffer, D. M., and B. A. Bekins (1998), Episodic fluid flow in the Nankai accretionary complex: Timescale, geochemistry, flow rates, and fluid budget, *J. Geophys. Res., 103*, 30,351–30,370.
Saffer, D. M., and C. Marone (2003), Comparison of smectite- and illite-rich gouge frictional properties: Application to the updip limit of the seismogenic zone along subduction megathrusts, *Earth Planet. Sci. Lett., 215*, 219–235.
Saffer, D. M., K. M. Frye, C. Marone, and K. Mir (2001), Laboratory results indicating complex and potentially unstable frictional behavior of smectite clay, *Geophys. Res. Lett., 28*, 2297–2300.
Satake, K. (1989), Inversion of tsunami waveforms for the estimation of heterogeneous fault motion of large submarine earthquakes: The 1968 Tokachi-oki and the 1983 Japan Sea earthquakes, *J. Geophys. Res., 94*, 5627–5636.
Satake, K. (1993), Depth distribution of coseismic slip along the Nankai Trough, Japan, from joint inversion of geodetic and tsunami data, *J. Geophys. Res., 98*, 4553–4565.
Satake, K. (1994), Mechanism of the 1992 Nicaragua tsunami earthquake, *Geophys. Res. Lett., 21*, 2519–2522.
Satake, K. (1995), Linear and nonlinear computations of the 1992 Nicaragua earthquake tsunami, *Pure Appl. Geophys., 144*, 455–470.
Satake, K., and Y. Tanioka (1999), Sources of tsunami and tsunamigenic earthquakes in subduction zones, *Pure Appl. Geophys., 154*, 467–483.
Satake, K., and Y. Tanioka (2003), The July 1998 Papua New Guinea earthquake: Mechanism and quantification of unusual tsunami generation, *Pure Appl. Geophys. 160*, 2087–2118.
Satake, K., J. Bourgeois, J., K. Abe, K. Abe, Y. Tsuji, F. Imamura, Y. Iio, H. Katao, E. Noguera, and F. Estrada, (1993), Tsunami field survey of the 1992 Nicaragua earthquake, *Eos Trans. AGU, 74*, 145, 156–157.
Sato, T., K. Imanishi, and M. Kosuga (1996), Three-stage rupture process of the 28 December 1994 Sanriku-oki earthquake, *Geophys. Res. Lett., 23*, 33–36.
Schindele, F., D. Reymond, E. Caucher, and E. Okal (1995), Analysis and automatic processing in near-field of eight 1992–1994 tsunamigenic earthquakes: Improvement towards real-time tsunami warning, *Pure Appl. Geophys. 144*, 381–408.
Scholz, C. (1990), *The Mechanics of Earthquakes and Faulting*, Cambridge Univ. Press, New York.
Scholz, C. (1998), Earthquakes and friction laws, *Nature, 391*, 37–42.
Scholz, C., and J. Campos (1995), On the mechanism of seismic decoupling and back arc spreading at subduction zones, *J. Geophys. Res., 100*, 22,103–22,115.

Scholz, C., and C. Small (1997), The effect of seamount subduction on seismic coupling, *Geology, 25*(6), 487–490.
Schwartz, S. Y., and L. J. Ruff (1985), The 1968 Tokachi-Oki and the 1969 Kurile Islands earthquakes: Variability in the rupture process, *J. Geophys. Res., 90*, 8613–8626.
Schwartz, S. Y., and L. J. Ruff (1987), Asperity distribution and earthquake occurrence in the southern Kurile Islands Arc, *Phys. Earth Planet. Int., 49*, 54–77.
Seno, T. (2000), The 21 September, 1999 Chi-Chi earthquake in Taiwan: Implications for tsunami earthquakes, *Terr. Atmos. Ocean Sci., 11*, 701–708.
Seno, T. (2002), Tsunami earthquakes as a transient phenomena, *Geophys. Res. Lett., 29*(10), 10.1029/2002Gl014868.
Shapiro, N. M., S. K. Singh, and J. Pacheco (1998), A fast and simple diagnostic method for identifying tsunamigenic earthquakes, *Geophys. Res. Lett., 25*, 3911–3914.
Shreve, R. L., and M. Cloos (1986), Dynamics of sediment subduction, melange, formation, and prism accretion, *J. Geophys. Res., 91*, 10, 229–10,245.
Suárez, G., and O. Sánchez (1996), Shallow depth of seismogenic coupling in southern Mexico: Implications for the maximum size of earthquakes in the subduction zone, *Phys. Earth Planet. Inter., 93*, 53–61.
Sykes, L. (1971), Aftershock zones of great earthquakes, seismicity gaps, and earthquake prediction for Alaska and the Aleutians, *J. Geophys. Res., 76*, 8021–8041.
Synolakis, C., P. Liu, G. Carrier, and Y. Yeh (1997), Tsunamigenic seafloor deformations, *Science, 278*, 598–600.
Synolakis, C. E., J. P. Bardet, J. C. Borrero, H. L. Davies, E. A. Okal, E. A. Silver, S. Sweet, and D. R. Tappin (2002), The slump origin of the 1998 Papua New Guinea tsunami, *Proc. R. Soc. London, 458*, 763–789.
Takahasi, N., S. Kodaira, T. Tsuru, J. Park, Y. Kaneda, H. Kinoshita, S. Abe, M. Nishino, and R. Hino (2000), Detailed plate boundary structure off northeast Japan coast, *Geophys. Res. Lett., 27*, 1977–1980.
Tanioka, Y. (1999), Analysis of the far-field tsunamis generated by the 1998 Papua New Guinea earthquake, *Geophys. Res. Lett., 26*, 3393–3396.
Tanioka, Y., and L. J. Ruff (1997), Source time functions, *Seismol. Res. Lett., 68*, 386–400.
Tanioka, Y., and K. Satake (1996a), Fault parameters of the 1896 Sanriku tsunami earthquake estimated from tsunami numerical modeling, *Geophys. Res. Lett., 23*, 1549–1552.
Tanioka, Y., and K. Satake (1996b), Tsunami generation by horizontal displacement of ocean bottom, *Geophys. Res. Lett., 23*, 861–864.
Tanioka, Y., and K. Satake (2001a), Coseismic slip distribution of the 1946 Nankai earthquake and aseismic slips caused by the earthquake, *Earth Planets Space, 53*, 235–241.
Tanioka, Y., and K. Satake (2001b), Detailed coseismic slip distribution of the 1944 Tonankai earthquake estimated from tsunami waveforms, *Geophys. Res. Lett., 28*, 1075–1078.
Tanioka, Y., and T. Seno (2001), The sediment effect on tsunami generation of the 1896 Sanriku tsunami earthquake, *Geophys. Res. Lett., 28*, 3389–3392.
Tanioka, Y., L. Ruff, and K. Satake (1996), The Sanriku-Oki, Japan, earthquake of December 28, 1994 (M_w 7.7): Rupture of a different asperity from a previous earthquake, *Geophys. Res. Lett., 23*, 1465–1468.
Tanioka, Y., L. Ruff, and K. Satake (1997), What controls the lateral variation of large earthquake occurrence along the Japan trench? *Island Arc, 6*, 261–266.
Tappin, D. R., et al. (1999), Sediment slump likely caused 1998 Papua New Guinea tsunami, *Eos Trans. AGU, 80*, 329–340.
Thatcher, W. (1989), Earthquake recurrence and risk assessment in circum-Pacific seismic gaps, *Nature, 341*, 432–434.
Thatcher, W. (1990), Order and diversity in the modes of circum-Pacific earthquake recurrence, *J. Geophys. Res., 95*, 2609–2623.

Tichelaar, B. W., and L. J. Ruff (1991), Seismic coupling along the Chilean subduction zone, *J. Geophys. Res., 96*, 11,997–12,022.

Tichelaar, B. W., and L. J. Ruff (1993), Depth of seismic coupling along subduction zones, *J. Geophys. Res., 98*, 2017–2037.

Titov, V. V., and C. E. Synolakis (1993), A numerical study of wave runup of the September 2, 1992 Nicaraguan tsunami, in *Proceedings of the IUGG/IOC International Tsunami Symposium*, Int. Union Geodesy and Geophysics, Intergov. Oceanographic Commission, Boulder, CO, pp. 627–635.

Tobin, H. J., J. C. Moore, and G. F. Moore (1994), Fluid pressure in the frontal thrust of the Oregon accretionary prism: Experimental constraints, *Geology, 22*(11), 979–982.

Tse, S. T., and J. R. Rice (1986), Crustal earthquake instability in relation to the depth variation of frictional slip properties, *J. Geophys. Res., 91*, 9452–9472.

Tsuji, Y., F. Imamura, H. Matsutomi, C. E. Synolakis, P. T. Nanang Jamadi, S. Harada, S. Han, K. Arai, and B. Cook (1995a), Field survey of the East Java earthquake and tsunami of June 3, 1994, *Pure Appl. Geophys., 144*, 839–854.

Tsuji, Y., H. Matsutomi, F. Imammura, M. Takeo, Y. Kawata, M. Matsuyama, T. Takahashi, and P. Sunarjo Harjadi (1995b), Damage to coastal villages due to the 1992 Flores island earthquake tsunami, *Pure Appl. Geophys., 144*, 481–524.

Uchida, N., T. Matsuzawa, A. Hasegawa, and T. Igarashi (2003), Interplate quasi-static slip off Sanriku, NE Japan, estimated from repeating earthquakes, *Geophys. Res. Lett., 30*(15), 1801, doi:10.1029/2003GL017452.

Umino, N., A. Hasegawa, and T. Matsuzawa (1995), sP depth phase at small epicentral distances and estimated subducting plate boundary, *Geophys. J. Int., 120*, 356–366.

Uyeda, S., and H. Kanamori (1979), Back-arc opening and the mode of subduction, *J. Geophys. Res., 84*, 1049–1061.

van der Hilst, R., and T. Seno (1993), Effects of relative plate motion on the deep structure and penetration depth of slabs below the Izu-Bonin and Mariana island arcs, *Earth Planet. Sci. Lett., 120*, 395–407.

Velasco, A., C. Ammon, T. Lay, and J. Zhang (1994), Imaging a slow bilateral rupture with broadband seismic waves: The September 2, 1992 Nicaraguan tsunami earthquake, *Geophys. Res., Lett., 21*, 2629–2632.

von Huene, R., and D. W. Scholl (1991), Observations at convergent margins concerning sediment subduction, subduction erosion, and the growth of continental crust, *Rev. Geophys., 29*, 279–316.

von Huene, R., D. Klaeschen, and J. Fruehn (1999), Relation between the subducting plate and seismicity associated with the great 1964 Alaska earthquake, *Pure Appl. Geophys., 154*, 575–591.

Vrolijk, P. (1990), On the mechanical role of smectite in subduction zones, *Geology, 18*(8), 703–707.

Ward, S. (1982), Earthquake mechanisms and tsunami generation: The Kurile Islands event of 13 October, 1963, *Bull. Seismol. Soc. Am., 72*, 759–777.

Wessel, P., and W. H. F. Smith (1991), Free software helps map and display data, *Eos Trans. AGU, 72*, 441–445.

Yagi, Y., M. Kikuchi, and T. Nishimura (2003), Co-seismic slip, post-seismic slip, and largest aftershock associated with the 1994 Sanriku-haruka-oki, Japan, earthquake, *Geophys. Res. Lett., 30*(22), 2177, doi:10.1029/2003GL018189.

Yoshii, T. (1979), A detailed cross-section of the deep seismic zone beneath northeastern Honshu, Japan, *Tectonophysics, 55*, 349–360.

Zhang, Z., and S. Y. Schwartz (1992), Depth distribution of moment release in underthrusting earthquakes at subduction zones, *J. Geophys. Res., 97*, 537–544.

Zobin, V. M. (1999), Changes in earthquake source properties across a shallow subduction zone: Kamchatka peninsula, *Pure Appl. Geophys., 154*, 457–466.